

Predicting properties of quantum thermal states from a single trajectory

Jiaqing Jiang^{1,†}, Jiaqi Leng^{1,2,†}, and Lin Lin^{2,3,*}

¹Simons Institute for the Theory of Computing, University of California, Berkeley,
USA

²Department of Mathematics, University of California, Berkeley, USA

³Applied Mathematics and Computational Research Division, Lawrence Berkeley
National Laboratory, Berkeley, USA

February 16, 2026

Abstract

Estimating thermal expectation values of observables is a fundamental task in quantum physics, quantum chemistry, and materials science. While recent quantum algorithms have enabled efficient quantum preparation of thermal states, observable estimation via sampling remains costly: a straightforward implementation separates successive measurements by a full mixing time in order to ensure samples are approximately independent. In this work, we show that the sampling cost can be substantially reduced by using a single Gibbs-sampling trajectory. After a single burn-in period, we interleave coherent measurements that satisfy detailed balance with respect to the target Gibbs state. The efficiency of this approach rests on the fact that, in many settings, the autocorrelation time can be significantly shorter than the mixing time. For energy estimation (and more generally for observables commuting with the Hamiltonian), we implement the required measurements using Gaussian-filtered quantum phase estimation with only logarithmic overhead. We also introduce a weighted operator Fourier transform technique to mitigate measurement-induced disturbance for general observables.

Contents

1	Introduction	2
1.1	Energy estimation from a single trajectory	2
1.2	Two challenges and our strategy	5
1.3	Examples of mixing time and autocorrelation time comparison	6
1.4	Outlook	8
2	Preliminaries and Notation	8
3	Goal and the proposed algorithm	10
4	Detailed-balanced measurements do not decrease the spectral gap	10
5	Time average behavior of Algorithm 1	12
5.1	Eigenfunctions and spectral covariance weight	12
5.2	Mixing Time, Relaxation Time, and Autocorrelation Time	13
5.3	Stationary moment identities	14
5.4	Reduction from arbitrary initialization	15
5.5	Time average behavior of the empirical average	16
5.6	Bounding autocorrelation time by the reciprocal spectral gap	16

[†]These authors contributed equally to this work.

*linlin@math.berkeley.edu

6 Implementation of the measurement	18
6.1 Gaussian-filtered quantum phase estimation (GQPE) and resource estimation	18
6.2 Detailed balanced measurement for commuting observables with low cost	19
6.3 Energy function estimation and cost comparison	20
6.4 Mitigating Measurement Disturbance for non-commuting observable via Operator Fourier Transform	22
A Proof of Theorem 6	24
B Quantum detailed balance and its property	26
C Examples for exponential decay of commutator norm	29
D Gaussian-filtered quantum phase estimation (GQPE)	30
D.1 Implementation for Idealized Gaussian Filtered quantum phase estimation	30
D.2 Circuit Implementation on qubits	31
D.3 Resource Estimation: Proof of Theorem 3	32

1 Introduction

Predicting the properties of quantum thermal states is a fundamental task in quantum many-body physics and is central to understanding the thermodynamic behavior of molecules and materials, including phase diagrams, binding energies, and response functions. Beyond physical simulations, thermal expectation estimation is also closely linked to quantum machine learning, for instance in training quantum Boltzmann machines that require efficient evaluation of gradients and expectation values [1, 2].

Recently, substantial progress has been made in dissipative quantum algorithms for preparing thermal states, including Lindblad dynamics [3, 4, 5], quantum Metropolis algorithm [6, 7, 8], and system–bath interaction methods [9, 10, 11]. These quantum algorithms can be viewed as quantum generalizations of Markov chain Monte Carlo (MCMC) methods, and offer a promising path toward predicting thermal properties of quantum systems, i.e., estimating expectation values of observables with respect to the Gibbs state. A straightforward sampling-based approach is to run multiple independent trajectories of a Gibbs-sampling algorithm and measure at the end of each trajectory; because measurements disturb the system, two consecutive measurements along a single trajectory may need to be separated by a time comparable to the mixing time (the worst-case time required to drive an arbitrary initial state close to stationarity) to ensure that the resulting samples are approximately independent. In this work, we show that this Gibbs-sampling cost can be significantly reduced: using a single trajectory, one can obtain effectively independent samples on a timescale that can be much shorter than the mixing time (for the observable of interest), enabling a more efficient method for observable estimation.

At the heart of this reduction is the notion of *autocorrelation time* [12], which is a standard concept in classical MCMC. In classical simulation, a common practice [13] is to run a single chain, first performing a warm-up (or *burn-in*) until the chain is close to stationarity, and then to collect samples spaced so that successive samples are effectively independent for the observable of interest. The autocorrelation time quantifies this spacing, and can be much smaller than the mixing time.

In the following, we focus first on estimating the average energy of quantum thermal states to highlight the challenges, intuitions, and strategies for using a single trajectory to estimate observable values in the quantum setting. We then discuss how the approach extends to observables whose estimation can be implemented in a thermodynamically reversible manner (i.e., via an operation that satisfies detailed balance). We also investigate a weighted operator Fourier transform technique to mitigate disturbances when estimating more general observables.

1.1 Energy estimation from a single trajectory

To begin with, we introduce some notation. For a local Hamiltonian H and inverse temperature β , the thermal equilibrium state is defined as the Gibbs state $\rho_\beta := \exp(-\beta H)/Z_\beta$, where Z_β is the normalization factor known as the partition function. For concreteness, in this section, we focus on the task of estimating the average energy of the Gibbs state, i.e., $\text{tr}(H\rho_\beta)$. We denote the variance of H as $\text{var}_H := \text{tr}(H^2\rho_\beta) - \text{tr}(H\rho_\beta)^2$.

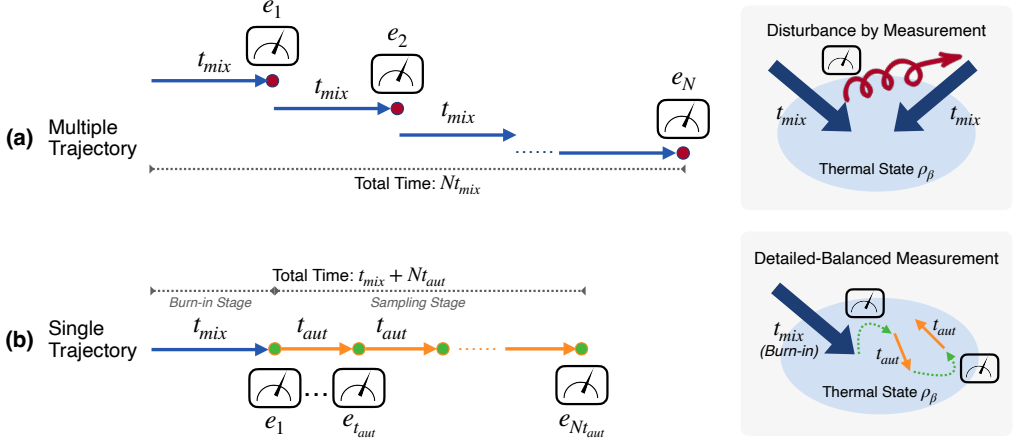


Figure 1: Two approaches for estimating $\text{tr}(H\rho_\beta)$ using a quantum Gibbs sampling algorithm (Gibbs sampling channel). (a) Multiple-trajectory approach: Run N independent trajectories, each applying the Gibbs sampling channel for the mixing time t_{mix} followed by a measurement of H . Conventionally, t_{mix} is used since quantum measurement collapses the state and may effectively reinitialize the Gibbs sampling dynamics. Estimating $\text{tr}(H\rho_\beta)$ to precision ϵ requires $N = \mathcal{O}(\text{var}_H / \epsilon^2)$. (b) Single-trajectory approach (this work): First, run a burn-in stage by applying the Gibbs sampling channel for the mixing time t_{mix} . Then, enter the sampling stage, where measurements are performed after each fixed evolution time Δt (a tunable parameter, set to $\Delta t = 1$ for simplicity). Measurements are chosen to satisfy detailed balance, implemented via Gaussian-filtered QPE, thus preserving the Gibbs state ensemble and avoiding extra burn-in periods. In this approach, effectively independent samples are obtained approximately every autocorrelation time t_{aut} . The autocorrelation time leverages a warm start from the previous measurement and depends on the observable of interest, and can therefore be much shorter than the mixing time. As a result, the total Gibbs sampling evolution time needed is $t_{mix} + Nt_{aut}$, which is significantly smaller than the Nt_{mix} required in the multiple-trajectory approach.

Multiple-trajectory approach As illustrated in Fig. 1(a), a straightforward way to estimate $\text{tr}(H\rho_\beta)$ using a Gibbs sampling algorithm is to run multiple independent trajectories. Each trajectory evolves for the mixing time t_{mix} . These trajectories then yield independent samples from which the average energy can be estimated. To achieve ϵ -precise estimation of $\text{tr}(H\rho_\beta)$, it suffices to run $N = \mathcal{O}(\text{var}_H / \epsilon^2)$ independent trajectories. Equivalently, this multi-trajectory procedure can be viewed as running a single long trajectory in which consecutive samples are separated by t_{mix} , where t_{mix} is conventionally used since a quantum measurement collapses the state and may effectively reinitialize the Gibbs sampling dynamics.

Single-trajectory approach Instead of separating samples by the full mixing time t_{mix} , as in Fig. 1(b), we use a two-stage algorithm to estimate $\text{tr}(H\rho_\beta)$. Starting from an arbitrary initial state, our algorithm proceeds as follows:

- (1) We first perform a *burn-in stage*, during which the Gibbs sampling channel is applied for one mixing time, allowing the chain to become approximately stationary, i.e., making the current state close to the Gibbs state.
- (2) We then proceed to the *sampling stage*, where measurements are performed after each fixed evolution time Δt along the trajectory. Note that the measurements are chosen to satisfy detailed balance, implemented via Gaussian-filtered quantum phase estimation (GQPE, explained later), *ensuring that during the sampling stage the chain remains in the Gibbs state ensemble* so that no additional burn-in is required. The evolution time Δt between successive measurements is treated as a tunable parameter. For simplicity we set $\Delta t = 1$.

Denoting the outcome of the j -th measurement as e_j , we estimate $\text{tr}(H\rho_\beta)$ as the empirical average of these outcomes along the trajectory, that is,

$$X_K := \frac{1}{K}(e_1 + \dots + e_K). \quad (1)$$

To build intuition, note that when H is a classical Hamiltonian like the Ising model, the Gibbs-sampling algorithm reduces to a classical Markov chain over the computational basis, and e_j is simply the energy of the current configuration.

This two-stage approach is widely used in classical MCMC and can substantially reduce the Gibbs sampling costs in practice. By the ergodic theorem for classical Markov chains, the empirical average X_K converges to $\text{tr}(H\rho_\beta)$, with the convergence rate determined by how quickly the samples $\{e_j\}_j$ become effectively independent — a timescale known as the *autocorrelation time*. The key observation that leads to the Gibbs sampling reduction is that the autocorrelation time can be much smaller than the mixing time, for two intuitive reasons. First, the autocorrelation time is an equilibrium notion, which quantifies decorrelation once the chain is already in stationarity. In contrast, the mixing time measures the *worst-case time* required to drive an arbitrary initial state to the Gibbs distribution. Second, the autocorrelation time is *observable-dependent*, and can therefore be shorter than the mixing time for observables that are local or exhibit certain symmetries. To build intuition, in Section 1.3 we provide examples where the autocorrelation time can be substantially smaller than the mixing time. More generally, for reversible classical Markov chains, the autocorrelation time can be bounded by the inverse spectral gap, while mixing-time bounds typically include an additional factor of order $\log(\pi_{\min}^{-1})$ [14]. In many models this factor scales linearly in the system size. In specific systems, the separation can be even more dramatic: for example, for low-temperature Glauber dynamics of the 2D Ising model, the mixing time can be sub-exponential in the system size [15], with scaling of the form $\exp(\Theta(\sqrt{n}))$ for n spins [15]; while existing literature [12, 16, 17] suggests that the autocorrelation time for the energy, which is symmetric under global spin flips, might grow at most polynomially with system size.

Despite the success in classical MCMC, however, it is not obvious that the same two-stage strategy also works well when applied to quantum Gibbs sampling without incurring significant overhead. In the following section, we outline the two main challenges and summarize our observations and strategies for addressing them. In particular, we formalize the notion of autocorrelation time for quantum Gibbs sampling and establish an upper bound in terms of the spectral gap of the underlying quantum Gibbs sampler, as summarized in the following:

Theorem 1 (Informal) *The autocorrelation time t_{aut} in the single-trajectory algorithm in Fig. 1 is upper bounded by the reciprocal of the spectral gap of the Gibbs sampler. To estimate $\text{tr}(H\rho_\beta)$ to precision ϵ with high probability, it suffices to take*

$$K = Nt_{\text{aut}}, \quad \text{for } N = \mathcal{O}(\text{var}_H/\epsilon^2). \quad (2)$$

Consequently, the total Gibbs sampling evolution time, $t_{\text{mix}} + Nt_{\text{aut}}$, can be much smaller than Nt_{mix} , substantially reducing the Gibbs sampling cost. Moreover, each measurement in our single-trajectory algorithm requires only a logarithmic number of ancilla qubits and logarithmic-time controlled Hamiltonian evolution of H , where the logarithmic scaling is with respect to both the precision ϵ and the spectral norm $\|H\|$.

Theorem 1 can be generalized to any observable that commutes with H , such as H^k . Formal statements are provided in Lemma 9, Theorem 2 and Theorem 5. The total cost of implementing measurements can be reduced by skipping unnecessary measurements, as discussed in Section 5 and Remark 1.

Practical implementation We remark that our algorithm can also be made *agnostic*, i.e., without prior knowledge of the mixing time or autocorrelation time. In applications where reliable estimates of these times are unavailable, one can run the burn-in period for an arbitrary fixed time T_{burn} , then enter the sampling period and take measurements after every fixed evolution time Δt . The empirical average along the trajectory, $(e_1 + \dots + e_K)/K$, still converges to the observable value $\text{tr}(H\rho_\beta)$, albeit at a slower rate due to the biased samples collected before the chain reaches stationarity.

In practice, one can monitor the empirical average along the Gibbs sampling trajectory and stop once it converges. In this sense, the agnostic version of our algorithm can be used as an empirical method for certifying the convergence of quantum Gibbs sampling, analogous to the Gelman–Rubin diagnostic used to assess convergence in classical MCMC [18, 19]. To our knowledge, no similar diagnostic protocol exists for certifying the convergence of quantum Gibbs sampling in the current literature; the only related work we are aware of certifies convergence for certain quantum Markov chains using a coupling-from-the-past technique [20].

1.2 Two challenges and our strategy

To help better understand Theorem 1, in this section we discuss two main challenges encountered when estimating $\text{tr}(H\rho_\beta)$ from a single trajectory, and explain how we address them.

First challenge: Disturbance from measurement The first challenge is that, unlike in classical Gibbs sampling, where evaluating $e_j = \langle x_j | H | x_j \rangle$ simply queries the current configuration $|x_j\rangle$ and leaves the Markov chain untouched, any intermediate measurement performed during quantum Gibbs sampling inevitably interferes with the sampling process. This interference occurs even if we assume that H can be measured perfectly in its eigenbasis. The reason is that in many quantum Gibbs sampling algorithms [3, 4], the transitions (or “jumps”) between intermediate states are highly entangling. Even if the system begins in an eigenstate of H , the application of a single update step typically produces a state that is a superposition of many energy eigenstates, often spanning a non-negligible energy range. Measuring the system in the energy eigenbasis at such an intermediate step collapses the superposition and therefore disrupts the intended evolution of the quantum Gibbs sampler. Consequently, inserting measurements can potentially increase the autocorrelation time, introducing an undesirable overhead. It is not even immediately clear whether inserting measurements necessarily worsens the mixing time; that is, the mixing time of the Gibbs sampler composed with a measurement channel could in principle be larger than that of the original Gibbs sampler.

We observe that although intermediate measurements inevitably disturb the Gibbs-sampling dynamics, their effect on the mixing time can be controlled when the measurement is compatible with the Gibbs state. In this case, one can show that the spectral gap of the Gibbs sampler composed with the measurement is never smaller than that of the original Gibbs sampler. Intuitively, the required compatibility condition is that the measurement leaves the Gibbs state unchanged, so no bias is introduced and no additional burn-in period is needed. Technically, the analysis requires a slightly stronger condition, namely, *detailed balance*, meaning that the measurement channel is thermodynamically reversible. In the specific task of estimating the energy $\text{tr}(H\rho_\beta)$, this compatibility condition is naturally satisfied when performing a coherent measurement of H , for instance through quantum phase estimation. To avoid confusion, we emphasize that even if the measurement fixes the Gibbs state, one must still evolve under the Gibbs-sampling channel for one autocorrelation time to obtain effectively *independent* samples. In summary, we prove that

Lemma 1 (Informal) *Let \mathcal{N} denote a quantum Gibbs-sampling channel that satisfies detailed balance, such as those constructed in [3, 4]. Let \mathcal{M} be a measurement channel that also satisfies detailed balance with respect to ρ_β . Then the spectral gap of the composed channel $\mathcal{M}\mathcal{N}\mathcal{M}$ is at least as large as the spectral gap of \mathcal{N} . Moreover, the autocorrelation time is upper bounded by (up to a small factor) the relaxation time of the Gibbs sampling channel, i.e., the reciprocal of the spectral gap of \mathcal{N} .*

A fully formal version of the above lemma appears in Lemma 3 and Lemma 9.

Second challenge: High cost of QPE The second challenge is that high-precision coherent quantum measurements can be costly, potentially erasing any advantage gained by replacing the mixing time with the autocorrelation time. In particular, implementing an ϵ -precision quantum phase estimation (QPE) algorithm for H requires a cost scaling of at least $\|H\|/\epsilon$ [21, 22, 23]. For local Hamiltonians written as a sum of κ bounded-norm terms, one typically has $\|H\| = \mathcal{O}(\kappa)$. In contrast, in classical Gibbs sampling, evaluating $\langle x_j | H | x_j \rangle$ exactly incurs a cost that is only linear in κ without the additional $1/\epsilon$ overhead.

To address this issue, we observe that high-precision coherent measurements are unnecessary: it suffices to use a coherent measurement that is *unbiased*. The key insight is that an unbiased measurement is sufficient because many samples are collected along the trajectory anyway. For measuring the energy $\text{tr}(H\rho_\beta)$ (or more generally any observable that commutes with H), we show that such a measurement can be implemented with only $\log(1/\epsilon)$ overhead relative to classical Gibbs sampling, in contrast to the $1/\epsilon$ overhead required for high-precision QPE.

Specifically, we construct the measurement from Gaussian-filtered QPE with adjustable variance (GQPE), as introduced in [24]. In particular, we set the variance of this GQPE to be of order one, which only slightly increases the variance of measuring ρ_β , i.e. var_H , by a constant, while significantly reducing the measurement overhead from $1/\epsilon$ to $\log(1/\epsilon)$. For concreteness, Table 1 provides a detailed comparison of the costs incurred by different methods of measuring H . Further

details on this comparison can be found in Section 6.3. We present a rigorous resource analysis of GQPE in Section 6.1, which, to our knowledge, is not available in prior literature and may be of independent interest.

Hamiltonian H	Measurement \mathcal{M}	Gate count $c_{\mathcal{M}}$	Depth $d_{\mathcal{M}}$	Variance $\text{var}_{\mathcal{M}}$	Total gate $c_{\mathcal{M}} \times \text{var}_{\mathcal{M}}$	Total depth $d_{\mathcal{M}} \times \text{var}_{\mathcal{M}}$
Classical	HP	n	1	n	n^2	n
	HP QPE	$n\epsilon^{-1}$	ϵ^{-1}	n	$n^2\epsilon^{-1}$	$n\epsilon^{-1}$
	*local	1	1	n^2	n^2	n^2
Quantum	GQPE	n	1	\mathbf{n}	\mathbf{n}^2	\mathbf{n}

Table 1: Comparison of costs for different methods of measuring H . To make meaningful comparison of circuit depth here we assume H is an n -qubit Hamiltonian on a 2D lattice. Gate and depth costs of a single measurement are denoted by $c_{\mathcal{M}}$ and $d_{\mathcal{M}}$, and $\text{var}_{\mathcal{M}}$ is the measurement variance w.r.t. ρ_{β} . The variance scalings shown in the table are schematic and model-dependent (they can change with temperature and correlations). Entries suppress a polylog($n\epsilon^{-1}$) factor, e.g., n represents $\mathcal{O}(n \text{polylog}(n\epsilon^{-1}))$. Measurement channels include: (HP) exact classical evaluation of $\langle x_j | H | x_j \rangle$; (HP QPE) high-precision QPE; (*local) measuring a randomly selected local term, here * represents that the measurement is non-coherent and significantly disturbs the Gibbs state; (GQPE) Gaussian-filtered QPE adapted in this work. The key quantities of interest are (1) the variance $\text{var}_{\mathcal{M}}$, which determines the number of samples need to be taken thus determine the total evolution time of the Gibbs-sampling channel; (2) the total gate and depth costs, $c_{\mathcal{M}} \times \text{var}_{\mathcal{M}}$ and $d_{\mathcal{M}} \times \text{var}_{\mathcal{M}}$, which determines the cost of implementing the measurement. GQPE achieves the lowest costs up to a polylog factor for all the three quantities of interest.

Mitigating measurement-induced disturbance for general observables From the previous sections, the *intuition* behind the two-stage algorithm in Fig. 1 is as follows: if a measurement leaves the Gibbs state ensemble unchanged, no additional burn-in is required during the sampling stage, potentially reducing the overall Gibbs sampling cost. This property generally does not hold for observables that do not commute with the Hamiltonian H : estimating $\text{tr}(O\rho_{\beta})$ via a projective measurement of O can significantly disturb the state away from ρ_{β} .

In Section 6.4, we take a first step toward mitigating this disturbance by exploring a weighted operator Fourier transform (WOFT) technique [25]. Roughly speaking, for a small parameter $\tau > 0$, WOFT constructs an observable $\hat{O}(\tau)$ that nearly commutes with ρ_{β} (equivalently, with H); that is, the commutator $[\hat{O}(\tau), \rho_{\beta}]$ approaches zero as $\tau \rightarrow 0$. Moreover, it is guaranteed that $\text{tr}(\rho_{\beta}\hat{O}(\tau)) = \text{tr}(\rho_{\beta}O)$. Therefore, to estimate $\text{tr}(\rho_{\beta}O)$, it suffices to measure the observable $\hat{O}(\tau)$, which nearly commutes with ρ_{β} . As a result of this near-commutation property, we show that measuring $\hat{O}(\tau)$ via GQPE perturbs ρ_{β} only slightly.

We note that although GQPE measurement for $\hat{O}(\tau)$ perturbs the Gibbs state only slightly when τ is sufficiently small, implementing this measurement could incur a higher cost than the logarithmic overhead achieved previously for observables that commute with H , unless additional assumptions are introduced. Besides, our analysis for bounding the autocorrelation time does not directly apply since this measurement does not satisfy *exact* detailed balance, though approximately fixes the Gibbs state.

1.3 Examples of mixing time and autocorrelation time comparison

We give examples in which the autocorrelation time of a fixed observable is much smaller than the mixing time. The reason is that the mixing time is a worst-case convergence time to the Gibbs state, whereas the autocorrelation time characterizes the decay of temporal correlations of an observable when the chain is started in stationarity (i.e., a warm start). In addition, the autocorrelation time is observable-dependent, and can be much smaller for observables that are insensitive to certain slow modes of the dynamics.

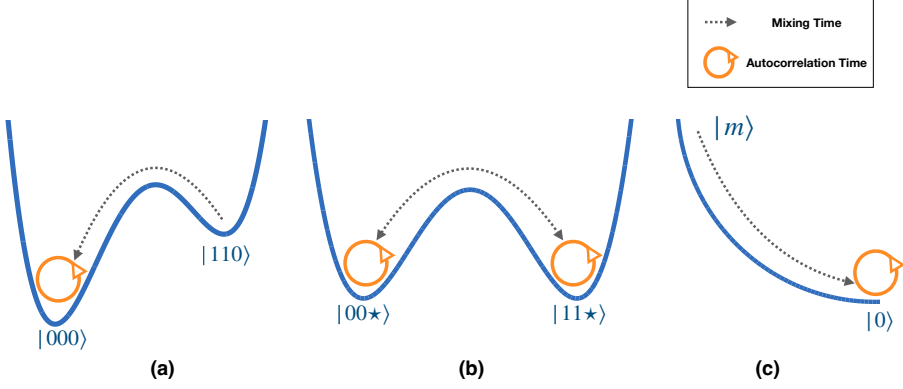


Figure 2: Three examples illustrating that the autocorrelation time of the energy observable can be much smaller than the mixing time. Let β be a constant inverse temperature. (a)(b) correspond to the three-qubit Ising model $H = -\alpha Z_1 Z_2 - h(Z_1 + Z_2) - \gamma Z_3$ under Glauber dynamics: (a) Asymmetric double-well ($\alpha \gg h \gg \gamma > 0$) with negligible Gibbs weight in the smaller well; the mixing time is $\Omega(e^{\beta\alpha})$ since transitions between the two wells require overcoming an energy barrier of order α , while the autocorrelation time is $\mathcal{O}(1)$ because typical stationary samples lie in the dominant well. (b) Symmetric double-well ($h = 0$ and $\gamma > 0$); the mixing time is $\Omega(e^{\beta\alpha})$, while the autocorrelation time is $\mathcal{O}(1)$ because the energy does not distinguish the two wells and its dominant fluctuations come from the decoupled spin Z_3 . (c) A classical birth-death chain on $|0\rangle, \dots, |m\rangle$; the mixing time scales as $\Omega(m)$, since starting from $|m\rangle$ the chain requires $\Omega(m)$ time to reach the low-energy states, whereas the autocorrelation time is $\mathcal{O}(1)$ since the Gibbs distribution is heavily concentrated near the low-energy states.

In Fig. 2(a)(b), we consider a three-qubit Ising model with external magnetic fields,

$$H = -\alpha Z_1 Z_2 - h(Z_1 + Z_2) - \gamma Z_3, \quad (3)$$

Here Z_i denotes the Pauli- Z operator acting on qubit i . The Gibbs sampling algorithm considered here is the (single-spin-flip) Glauber dynamics: at each step, a spin is chosen uniformly at random and flipped with probability $\min\{1, e^{-\beta\Delta}\}$, where Δ denotes the energy difference between the configurations before and after the spin flip. Here $\alpha, h, \gamma \geq 0$. Suppose our goal is to estimate $\text{tr}(H\rho_\beta)$ to finite precision, e.g., $\epsilon = 10^{-6}$.

In the regime $\alpha \gg h \gg \gamma > 0$, as in Fig. 2(a), the Hamiltonian in Eq. (3) forms an asymmetric double-well landscape: the global minimum $|000\rangle$ lies in the dominant well, and a local minimum $|110\rangle$ lies in the smaller well. The Gibbs probabilities of these minima differ exponentially,

$$\frac{\text{Pr}[|000\rangle]}{\text{Pr}[|110\rangle]} = e^{4\beta h}.$$

For example, with $\beta = 5$ and $h = 1$, one has $\exp(4\beta h) \approx 10^8$.

Under Glauber dynamics, escaping the smaller well requires overcoming an energy barrier of order α , so the mixing time scales as $\Omega(e^{\beta\alpha})$. In contrast, the autocorrelation time is $\mathcal{O}(1)$ (treating γ as a constant), because the stationary distribution is concentrated in the dominant well. Quantitatively, relative to $|000\rangle$, the smaller-well minimum $|110\rangle$ is suppressed by a factor $e^{-4\beta h}$ (about $2 \cdot 10^{-9}$ for $\beta = 5$ and $h = 1$), while configurations with $Z_1 Z_2 = -1$ are further suppressed by at least $e^{-\beta(2\alpha+2h)}$. Hence, at accuracy $\epsilon = 10^{-6}$, stationary samples effectively remain in the dominant well, and the energy decorrelates on the constant timescale of local updates (in particular, rapid flips of the decoupled spin Z_3).

Let us also consider a different parameter regime $h = 0$ and $\gamma > 0$. As in Fig. 2(b), the Hamiltonian in Eq. (3) forms a symmetric double-well landscape in the $Z_1 Z_2$ degree of freedom, with two basins corresponding to $|00*\rangle$ and $|11*\rangle$; the global minima are $|000\rangle$ and $|110\rangle$.

Under Glauber dynamics, escaping one well to reach the other requires overcoming an energy barrier of order α , so the mixing time scales as $\Omega(e^{\beta\alpha})$. However, since the energy observable H does not distinguish the two wells (it depends on $Z_1 Z_2$ and Z_3), its autocorrelation time does not reflect the rare inter-well transitions. Instead, the autocorrelation time remains $\mathcal{O}(1)$ because the dominant energy fluctuations come from the local relaxation of the decoupled spin Z_3 (the $-\gamma Z_3$ term), which flips at a rate independent of the barrier between the $Z_1 Z_2$ configurations.

We remark that the same mechanisms can lead to a sub-exponential separation between the mixing time and the autocorrelation time. For instance, global mixing in the low-temperature 2D Ising model is sub-exponentially slow in the system size, with scaling of the form $\exp(\Theta(\sqrt{n}))$ for n spins [15]. Existing studies [12, 16, 17] suggest that the dynamics restricted to a single well (phase) can mix in polynomial time. This suggests that the autocorrelation time of the energy may grow at most polynomially, since the energy is a symmetric observable whose relaxation is dominated by rapid fluctuations within a single well (phase) rather than by exponentially slow tunneling between two wells.

Both Fig. 2(a) and (b) involve energy barriers. Finally, even without energy barriers, there can be a polynomial separation between mixing time and autocorrelation time (Fig. 2(c)). Consider a classical birth-death chain on states $|0\rangle, |1\rangle, \dots, |m\rangle$. The transition probabilities are defined as follows: from state $|k\rangle$, the chain transitions to $|k-1\rangle$ with probability p , and to $|k+1\rangle$ with probability q , where $p+q=1$, $\log(p/q)=\beta$ and $p>q$. At the boundaries, the chain transitions from $|0\rangle$ to $|1\rangle$ with probability q and stays at $|0\rangle$ with probability p , and transitions from $|m\rangle$ to $|m-1\rangle$ with probability p and stays at $|m\rangle$ with probability q . One can verify that the invariant distribution π is the Gibbs distribution, with $\pi_k \propto (q/p)^k = \exp(-\beta k)$. The mixing time is $\Omega(m)$, since starting from $|m\rangle$, reaching the ground state $|0\rangle$ requires at least m steps. In contrast, the autocorrelation time for the energy observable is $\mathcal{O}(1)$, since the spectral gap of this biased birth-death chain is $\mathcal{O}(1)$ (independent of m). Intuitively, the autocorrelation time is small because typical configurations sampled from the Gibbs distribution are concentrated near the ground state, providing an effective warm start for the autocorrelation dynamics.

1.4 Outlook

In this work, we introduce a framework for estimating quantum thermal expectation values using a single trajectory. For observables that can be measured in a thermodynamically reversible way (i.e., satisfying detailed balance), our approach achieves substantial reductions in sampling cost compared with multi-trajectory methods. The core of our approach is an extension of the notion of autocorrelation from classical Markov chain Monte Carlo to quantum Gibbs sampling, combined with a careful treatment of measurement to control the effects of measurement-induced disturbance.

An exciting direction is to generalize our framework to estimate thermal expectation values for general observables. Here, we investigate the idea of using weighted operator Fourier transform and show that, in certain cases, it can mitigate measurement-induced disturbances. It would be interesting to explore its effectiveness in more general settings through experiments or numerical simulations. Beyond the weighted operator Fourier transform idea, one could also explore methods for measuring general observables in a thermodynamically reversible manner, potentially linking to techniques that map general observables to detailed-balanced Lindbladians [25, 4]. Intuitions from discrete-time Metropolis algorithms may also provide useful guidance [6, 7, 8].

Given the wide success of the corresponding classical MCMC analogy, we expect our single-trajectory framework to have a broad practical impact. An important question for future work is how to accurately estimate the autocorrelation time and the resulting effective sample size, which could be explored through theoretical analysis or numerical simulations, similar to methods used in classical MCMC [12, 26, 27].

2 Preliminaries and Notation

Local Hamiltonian and Gibbs state We use $H = \sum_{i=1}^{\kappa} H_i$ to denote an n -qubit local Hamiltonian where $\kappa = \text{poly}(n)$ is the number of terms, each H_i acts nontrivially on at most $O(1)$ qubits, and $\|H_i\| \leq 1$. Given a local Hamiltonian H and inverse temperature β , the Gibbs state is defined as

$$\rho_{\beta} = \exp(-\beta H)/Z_{\beta}, \quad (4)$$

where $Z_{\beta} = \text{tr}(\exp(-\beta H))$ is the normalization factor.

Quantum channel and weighted inner product We use quantum channels to denote completely positive and trace preserving maps (CPTP). Let \mathcal{T} be a quantum channel with Kraus

operators $\{K_u\}_u$, i.e. $\mathcal{T}(\cdot) := \sum_u K_u(\cdot) K_u^\dagger$. The map in the Heisenberg picture is defined as

$$\mathcal{T}^\dagger(\cdot) := \sum_u K_u^\dagger(\cdot) K_u,$$

which is the dual map w.r.t. the Hilbert-Schmidt inner product $\langle A, B \rangle := \text{tr}(A^\dagger B)$.

For any $s \in [0, 1]$, the weighted inner product is defined as

$$\langle M, N \rangle_s := \text{tr}(M^\dagger \rho_\beta^{1-s} N \rho_\beta^s).$$

Quantum detailed balance and spectral gap. We say a quantum channel \mathcal{T} satisfies s -detailed balance (w.r.t. ρ_β) if, for any operators A and B , the map \mathcal{T}^\dagger is self-adjoint w.r.t. the weighted inner product,

$$\langle A, \mathcal{T}^\dagger(B) \rangle_s = \langle \mathcal{T}^\dagger(A), B \rangle_s.$$

When $s = \frac{1}{2}$ we say that \mathcal{T} satisfies KMS (Kubo-Martin-Schwinger) quantum detailed balance.

Fact 1 (Properties of quantum detailed balance) *Any quantum channel \mathcal{T} that satisfies s -detailed balance fixes the Gibbs state, i.e. $\mathcal{T}(\rho_\beta) = \rho_\beta$. Moreover,*

- \mathcal{T} is diagonalizable with a real spectrum contained in $[-1, 1]$. When \mathcal{T} arises from the time evolution of a Lindbladian, its spectrum is further restricted to $[0, 1]$.
- The spectrum of \mathcal{T}^\dagger is the complex conjugate of the spectrum of \mathcal{T} ; in particular, under s -detailed balance the spectrum is real and hence the spectra coincide.
- If \mathcal{T} has a unique fixed state and its spectrum is contained in $[0, 1]$ (e.g., when \mathcal{T} arises from the time evolution of a Lindbladian), then its spectral gap can be written as

$$\text{gap}(\mathcal{T}) = \text{gap}(\mathcal{T}^\dagger) = 1 - \max_{X \neq 0, \langle X, I \rangle_s = 0} \frac{\langle X, \mathcal{T}^\dagger(X) \rangle_s}{\langle X, X \rangle_s}. \quad (5)$$

For completeness, a proof of the above fact is provided in Appendix B Lemma 16.

Matrix norm. We use \mathbb{M} to denote the linear space formed by all $\mathbb{C}^{2^n \times 2^n}$ matrices. For any matrix $A \in \mathbb{M}$, we use $\|A\|_1$ and $\|A\|$ to denote its trace norm and operator norm respectively. For any two indices x and y , we use δ_{xy} to denote the function that equals 1 if $x = y$ and 0 otherwise.

Expectation, variance and covariance. Let \mathcal{P} be a quantum channel with Kraus operators $\{Q_u\}_u$, where the index set $\{u\}_u$ takes real values and denotes the possible measurement outcomes. In other words, \mathcal{P} is a quantum instrument with classical outcome u , so that $\sum_u Q_u^\dagger Q_u = I$.

Consider applying the quantum channel \mathcal{P} to a state ρ . We use $\mathbb{E}_\rho(\mathcal{P})$ and $\text{Var}_\rho(\mathcal{P})$ to denote the expectation and variance of the measurement outcomes, that is,

$$\mathbb{E}_\rho(\mathcal{P}) := \sum_u u \text{tr}(Q_u \rho Q_u^\dagger), \quad (6)$$

$$\text{Var}_\rho(\mathcal{P}) := \sum_u |u - \mathbb{E}_\rho(\mathcal{P})|^2 \text{tr}(Q_u \rho Q_u^\dagger). \quad (7)$$

The covariance of \mathcal{P} is defined as the correlation between the measurement outcomes of two successive measurements, corresponding to two successive applications of the same instrument with no intermediate evolution,

$$\text{Cov}_\rho(\mathcal{P}) := \sum_{x,y} (x - \mathbb{E}_\rho(\mathcal{P})) (y - \mathbb{E}_\rho(\mathcal{P})) \text{tr}(Q_y Q_x \rho Q_x^\dagger Q_y^\dagger). \quad (8)$$

Note that when \mathcal{P} corresponds to a projective measurement, i.e., $Q_x = Q_x^\dagger$ and $Q_x Q_y = \delta_{xy} Q_x$, we have $\text{Var}_\rho(\mathcal{P}) = \text{Cov}_\rho(\mathcal{P})$.

3 Goal and the proposed algorithm

In this paper, we study the problem of estimating thermal expectation values using an existing quantum Gibbs sampling algorithm as a subroutine.

More precisely, we assume that we have access to a quantum Gibbs sampling algorithm, modeled as a quantum channel \mathcal{N} that satisfies s -detailed balance and has ρ_β as its unique fixed state. We assume that the spectrum of \mathcal{N} lies in $[0, 1]$. The quantum Gibbs-sampling channel \mathcal{N} can be instantiated using known quantum Gibbs samplers [3, 4] that satisfy KMS detailed balance ($s = 1/2$), which are based on simulating Davies-generator-inspired Lindbladian \mathcal{L} . More specifically, one can set $\mathcal{N} := e^{t_0 \mathcal{L}}$ for any chosen $t_0 > 0$. In particular, the spectrum of those Lindbladian-based channels \mathcal{N} is contained in $[0, 1]$ by Fact 1.

Our goal and proposed algorithm. Our goal is to use \mathcal{N} as a subroutine to estimate $\text{tr}(O\rho_\beta)$ for a given observable O . We use \mathcal{M} to denote a quantum channel that implements the measurement of O , in the sense that, when applied to ρ_β , its measurement outcome has expectation value $\text{tr}(O\rho_\beta)$. The implementation of the measurement channel \mathcal{M} will be specified later in Section 6. For illustration, one may temporarily assume $O = H$ and interpret \mathcal{M} as a particular implementation of the quantum phase estimation algorithm.

As described in the introduction and shown in Figure 1 (b), we estimate observable values in quantum Gibbs sampling using a single trajectory, as outlined in Algorithm 1. For proof purposes, in line 3 of Algorithm 1, we apply the measurement \mathcal{M} twice rather than once. Additionally, Algorithm 1 is currently presented in a practical i.e., agnostic mode, where measurements are performed at fixed intervals; in Section 5.5, Remark 1 further discusses how the cost of measurements can be reduced by skipping unnecessary measurements.

Algorithm 1 Observable Estimation from a single trajectory

Inputs: Quantum channel \mathcal{N} and \mathcal{M} ; Initial state ρ ; Integers T_{burn} and K

- 1: Apply \mathcal{N} for time T_{burn} to the initial state ρ
- 2: **for** $t = 1$ to K **do**
- 3: Apply $\mathcal{E} := \mathcal{M} \circ \mathcal{N} \circ \mathcal{M}$
- 4: Denote the measurement outcome of the first \mathcal{M} (i.e., the rightmost \mathcal{M} in the composition defining \mathcal{E}) as e_t
- 5: **end for**
- 6: Output $X_K := \frac{1}{K} \sum_{t=1}^K e_t$

Structure of the manuscript. We will first assume that \mathcal{M} satisfies s -detailed balance and analyze the performance of Algorithm 1. In particular, in Section 4 we prove that detailed-balance measurements never decrease the spectral gap. In Section 5, we introduce the concept of autocorrelation time in quantum Gibbs sampling and bound it by the relaxation time multiplied by an additional factor, which will later be shown to be constant for our choice of \mathcal{M} .

Then we will explain the implementation of the measurement \mathcal{M} . In Section 6.2, we focus on operators O that commute with H and construct a measurement \mathcal{M} that is unbiased, satisfies s -detailed balance, and incurs only a logarithmic overhead. As an explicit example, in Section 6.3, we focus on measuring H and give a detailed comparison of the gate and depth complexity between different approaches of measuring H . Finally, we employ the operator Fourier transform technique to mitigate the measurement-induced disturbance for more general observables.

4 Detailed-balanced measurements do not decrease the spectral gap

In this section, we prove that detailed-balanced measurements do not decrease the spectral gap. First notice that the following lemma holds. Its proof is provided in Appendix B.

Lemma 2 *Let \mathcal{M} and \mathcal{N} be quantum channels satisfying s -detailed balance with respect to ρ_β ; then the composite channel $\mathcal{M}\mathcal{N}\mathcal{M}$ also satisfies s -detailed balance. Moreover, if \mathcal{N} has ρ_β as its*

unique fixed point and its spectrum is contained in $[0, 1]$, then $\mathcal{M}\mathcal{N}\mathcal{M}$ also has ρ_β as its unique fixed point and its spectrum lies in $[0, 1]$.

Now we are ready to state the lemma that connects the spectral gap of $\mathcal{M}\mathcal{N}\mathcal{M}$ and \mathcal{N} .

Lemma 3 *Consider two quantum channels \mathcal{M} and \mathcal{N} that satisfy s -detailed balance with respect to ρ_β . Suppose \mathcal{N} admits ρ_β as its unique fixed point and has spectrum contained in $[0, 1]$. Then we have that*

$$\text{gap}(\mathcal{M}\mathcal{N}\mathcal{M}) \geq \text{gap}(\mathcal{N}). \quad (9)$$

To prove Lemma 3, first notice that a detailed-balance channel is contractive under the weighted inner product.

Lemma 4 (Contractivity of a detailed-balance channel under the weighted norm) *Let \mathcal{T} be a quantum channel that satisfies s -detailed balance. Then, for any operator A , we have*

$$\langle A, A \rangle_s \geq \langle \mathcal{T}^\dagger(A), \mathcal{T}^\dagger(A) \rangle_s. \quad (10)$$

Proof: Since \mathcal{T} satisfies s -detailed balance, we have that \mathcal{T}^\dagger is Hermitian w.r.t. the weighted inner product $\langle \cdot, \cdot \rangle_s$. Thus, there exists an orthonormal basis of \mathbb{M} , that is, $\{Y_i\}_i \subseteq \mathbb{M}$ where $\langle Y_i, Y_j \rangle_s = \delta_{ij}$ such that $\mathcal{T}^\dagger(Y_i) = \lambda_i Y_i$. Since \mathcal{T}^\dagger is Hermitian w.r.t. $\langle \cdot, \cdot \rangle_s$, we have $\lambda_i \in \mathbb{R}$. Moreover, $|\lambda_i| \leq 1$ since \mathcal{T} is a quantum channel by Fact 1.

Since $\{Y_i\}_i$ forms a basis of \mathbb{M} , we can express the operator A w.r.t the eigenstates $\{Y_i\}_i$,

$$A = \sum_i a_i Y_i, \text{ where } a_i = \langle Y_i, A \rangle_s. \quad (11)$$

Then it suffices to notice that $|\lambda_i| \leq 1$ implies

$$\langle \mathcal{T}^\dagger(A), \mathcal{T}^\dagger(A) \rangle_s = \sum_i \lambda_i^2 |a_i|^2 \leq \sum_i |a_i|^2 = \langle A, A \rangle_s. \quad (12)$$

■

Now we are prepared to prove Lemma 3.

Proof: [of Lemma 3] From Lemma 2 we have that $\mathcal{M}\mathcal{N}\mathcal{M}$ has ρ_β as its unique fixed point and spectrum in $[0, 1]$. Since both \mathcal{M} and \mathcal{N} satisfy s -detailed balance, then so does $\mathcal{M}\mathcal{N}\mathcal{M}$, by the definition of spectral gap [Fact 1] we have that

$$\text{gap}(\mathcal{N}) = 1 - \max_{X \neq 0, \langle X, I \rangle_s = 0} \frac{\langle X, \mathcal{N}^\dagger(X) \rangle_s}{\langle X, X \rangle_s} \quad (13)$$

$$\leq 1 - \max_{X \neq 0, \langle \mathcal{M}^\dagger(X), I \rangle_s = 0} \frac{\langle \mathcal{M}^\dagger(X), \mathcal{N}^\dagger \mathcal{M}^\dagger(X) \rangle_s}{\langle \mathcal{M}^\dagger(X), \mathcal{M}^\dagger(X) \rangle_s}. \quad (14)$$

where the last inequality comes from restricting the maximization to the subset of test operators of the form $\mathcal{M}^\dagger(X)$. Note that \mathcal{M} is a quantum channel thus $\mathcal{M}^\dagger(I) = I$. Combine with the fact that \mathcal{M} satisfies s -detailed balance, we have

$$\langle \mathcal{M}^\dagger(X), I \rangle_s = \langle X, \mathcal{M}^\dagger(I) \rangle_s = \langle X, I \rangle_s, \quad (15)$$

$$\langle \mathcal{M}^\dagger(X), \mathcal{N}^\dagger \mathcal{M}^\dagger(X) \rangle_s = \langle X, \mathcal{M}^\dagger \mathcal{N}^\dagger \mathcal{M}^\dagger(X) \rangle_s \geq 0. \quad (16)$$

where the ≥ 0 comes from the fact that the spectrum of \mathcal{N}^\dagger lies in $[0, 1]$ since \mathcal{N} has spectrum in $[0, 1]$ [Fact 1]. Thus by Lemma 4 and Eq. (14), we have that

$$\text{gap}(\mathcal{N}) \leq 1 - \max_{X \neq 0, \langle X, I \rangle_s = 0} \frac{\langle X, \mathcal{M}^\dagger \mathcal{N}^\dagger \mathcal{M}^\dagger(X) \rangle_s}{\langle \mathcal{M}^\dagger(X), \mathcal{M}^\dagger(X) \rangle_s} \quad (17)$$

$$\leq 1 - \max_{X \neq 0, \langle X, I \rangle_s = 0} \frac{\langle X, \mathcal{M}^\dagger \mathcal{N}^\dagger \mathcal{M}^\dagger(X) \rangle_s}{\langle X, X \rangle_s} \quad (18)$$

$$= \text{gap}(\mathcal{M}\mathcal{N}\mathcal{M}). \quad (19)$$

■

5 Time average behavior of Algorithm 1

In this section, we analyze the performance of our single-trajectory observable estimation algorithm, Algorithm 1, under the assumption that the measurement \mathcal{M} satisfies s -detailed balance. Section 5.1 defines the spectral covariance weight and explains its relationship to the variance. In Section 5.2, we present the definitions of mixing time, relaxation time, and introduce the autocorrelation time in the context of quantum Gibbs sampling. Finally, Section 5.5 bounds the autocorrelation time and analyzes the behavior of time-averaged observable values along the trajectory.

We first introduce some notation that will be used throughout this section.

Channels and their eigenstates. In this section we consider applying Algorithm 1 with quantum channels \mathcal{N} and \mathcal{M} that satisfy the following properties.

Assumption 1 Consider two quantum channels \mathcal{N} and \mathcal{M} that satisfy s -detailed balance with respect to ρ_β . Suppose that \mathcal{N} has ρ_β as its unique fixed state and that its spectrum lies in $[0, 1]$.

As we discussed in Section 3, \mathcal{N} refers to quantum Gibbs samplers like [3, 4]. By Lemma 2, the composite channel $\mathcal{E} := \mathcal{M}\mathcal{N}\mathcal{M}$ also has ρ_β as its unique fixed state and its spectrum is contained in $[0, 1]$. Besides, \mathcal{E} also satisfies s -detailed balance, thus \mathcal{E}^\dagger is Hermitian w.r.t. the weighted inner product $\langle \cdot, \cdot \rangle_s$. Thus there exists a set of matrices $\{Y_i\}_i$ such that

- Orthonormal w.r.t weighted inner product: $\langle Y_i, Y_j \rangle_s = \delta_{ij}$.
- Basis: $\{Y_i\}_i$ forms a basis of \mathbb{M} .
- Eigenstate: $\mathcal{E}^\dagger(Y_i) = \lambda_i Y_i$, $\lambda_i \in [0, 1]$. In particular $Y_1 = I$ i.e. the identity matrix. Without loss of generality, we organize λ_i in non-increasing order $1 = \lambda_1 > \lambda_2 \geq \lambda_3 \dots$.

Expectation, Variance and Covariance Let \mathcal{P} be a quantum channel with Kraus operators $\{Q_u\}_u$, where the index set $\{u\}_u$ takes real values and denotes the possible measurement outcomes.

Consider applying \mathcal{P} to the Gibbs state ρ_β . As defined in the preliminary section (Section 2), we use $\mathbb{E}_{\rho_\beta}(\mathcal{P})$, $\text{Var}_{\rho_\beta}(\mathcal{P})$ and $\text{Cov}_{\rho_\beta}(\mathcal{P})$ to denote the expectation, variance, and covariance of the measurement \mathcal{P} .

Autocorrelation function For technical reasons, it is more convenient to treat $\mathcal{E} = \mathcal{M}\mathcal{N}\mathcal{M}$ as a single channel rather than analyze \mathcal{N} and \mathcal{M} separately. In particular, we regard \mathcal{E} as a measurement channel whose outcome is the outcome of the first application of \mathcal{M} , consistent with Algorithm 1.

Denote the Kraus operators of \mathcal{M} by $\{O_u\}_u$. Define the map that sends an operator to its measurement–outcome–weighted operator as follows:

$$\widehat{\mathcal{M}}(X) := \sum_u (u - \mathbb{E}_{\rho_\beta}(\mathcal{M})) O_u X O_u^\dagger, \quad (20)$$

$$\widehat{\mathcal{E}}(X) := \mathcal{M} \circ \mathcal{N} \circ \widehat{\mathcal{M}}(X). \quad (21)$$

The autocorrelation function of \mathcal{E} at time lag t is the correlation between the measurement outcomes at time steps 0 and $t + 1$:

$$\text{Corr}_{\rho_\beta}(\mathcal{E}^t) := \text{tr} \left(\widehat{\mathcal{E}} \circ \mathcal{E}^t \circ \widehat{\mathcal{E}}(\rho_\beta) \right). \quad (22)$$

In particular, $\text{Corr}_{\rho_\beta}(\mathcal{E}^0) = \text{tr} \left(\widehat{\mathcal{E}} \circ \widehat{\mathcal{E}}(\rho_\beta) \right)$.

5.1 Eigenfunctions and spectral covariance weight

Recall that $\{Y_i\}_i$ are eigenstates of \mathcal{E}^\dagger that form a basis of the operator space \mathbb{M} . To aid the proof, we express the map $\widehat{\mathcal{E}}^\dagger$ in terms of these eigenstates $\{Y_i\}_i$. That is, for any Y_i , we write

$$\widehat{\mathcal{E}}^\dagger(Y_i) = \sum_j \alpha_{ij} Y_j, \text{ where } \alpha_{ij} := \langle Y_j, \widehat{\mathcal{E}}^\dagger(Y_i) \rangle_s. \quad (23)$$

Recall that $Y_1 = I$. Note that $\mathcal{M}^\dagger(I) = I$ since \mathcal{M} is a quantum channel and similarly for \mathcal{N} .

Lemma 5 *We have $\alpha_{11} = 0$ since*

$$\alpha_{11} = \langle I, \widehat{\mathcal{M}}^\dagger \mathcal{N}^\dagger \mathcal{M}^\dagger(I) \rangle_s = \text{tr}(\rho_\beta \widehat{\mathcal{M}}^\dagger(I)) = \text{tr}(\widehat{\mathcal{M}}(\rho_\beta)) = 0.$$

We define the spectral covariance weight as

Definition 6 (Spectral covariance weight) *The spectral covariance weight of the map $\mathcal{E} = \mathcal{M} \mathcal{N} \mathcal{M}$ is defined as*

$$\mathbb{W}_{\rho_\beta}(\mathcal{E}) := \sum_j |\alpha_{1j} \alpha_{j1}|.$$

The spectral covariance weight will be used in Section 5.6 to bound the autocorrelation time in terms of the spectral properties of the Gibbs sampling channel, namely its spectral gap. Note that in the definition, α_{j1} might *not* equal to α_{1j}^* .

In the following, we show that when $\widehat{\mathcal{M}}$ also satisfies *s*-detailed balance, the spectral covariance weight of \mathcal{E} can be upper-bounded by the covariance of \mathcal{M} , which equals the variance of \mathcal{M} if \mathcal{M} is a projective measurement. To avoid confusion, we remark that for operators commuting with H , later in Section 6.2 we will explicitly implement a measurement \mathcal{M} such that both \mathcal{M} and $\widehat{\mathcal{M}}$ satisfy *s*-detailed balance.

Lemma 7 *Suppose the map $\widehat{\mathcal{M}}$ satisfies *s*-detailed balance, then*

$$\mathbb{W}_{\rho_\beta}(\mathcal{E}) \leq \text{Cov}_{\rho_\beta}(\mathcal{M}).$$

Proof: By Eq. (23), we have that

$$\sum_j |\alpha_{1j}|^2 = \langle \widehat{\mathcal{E}}^\dagger(I), \widehat{\mathcal{E}}^\dagger(I) \rangle_s = \langle \widehat{\mathcal{M}}^\dagger(I), \widehat{\mathcal{M}}^\dagger(I) \rangle_s \quad (24)$$

where we implicitly use $\mathcal{M}^\dagger(I) = I$, $\mathcal{N}^\dagger(I) = I$ since \mathcal{M} and \mathcal{N} are quantum channels.

Besides, since $\widehat{\mathcal{M}}$, \mathcal{M} and \mathcal{N} satisfy *s*-detailed balance, we have that

$$\alpha_{j1} = \langle I, \widehat{\mathcal{E}}^\dagger(Y_j) \rangle_s = \langle I, \widehat{\mathcal{M}}^\dagger \mathcal{N}^\dagger \mathcal{M}^\dagger(Y_j) \rangle_s = \langle \mathcal{M}^\dagger \mathcal{N}^\dagger \widehat{\mathcal{M}}^\dagger(I), Y_j \rangle_s, \quad (25)$$

$$\text{thus } \mathcal{M}^\dagger \mathcal{N}^\dagger \widehat{\mathcal{M}}^\dagger(I) = \sum_j \alpha_{j1}^* Y_j. \quad (26)$$

Thus we have

$$\sum_j |\alpha_{j1}|^2 = \langle \mathcal{M}^\dagger \mathcal{N}^\dagger \widehat{\mathcal{M}}^\dagger(I), \mathcal{M}^\dagger \mathcal{N}^\dagger \widehat{\mathcal{M}}^\dagger(I) \rangle_s \quad (27)$$

$$\leq \langle \mathcal{N}^\dagger \widehat{\mathcal{M}}^\dagger(I), \mathcal{N}^\dagger \widehat{\mathcal{M}}^\dagger(I) \rangle_s \quad (28)$$

$$\leq \langle \widehat{\mathcal{M}}^\dagger(I), \widehat{\mathcal{M}}^\dagger(I) \rangle_s \quad (29)$$

where for the last two inequalities we use the fact that since \mathcal{M} , \mathcal{N} satisfy *s*-detailed balance, then \mathcal{M}^\dagger and \mathcal{N}^\dagger are contractive w.r.t. weighted norm [Lemma 4]. Besides, since $\widehat{\mathcal{M}}$ satisfies *s*-detailed balance, we further have that

$$\langle \widehat{\mathcal{M}}^\dagger(I), \widehat{\mathcal{M}}^\dagger(I) \rangle_s = \langle I, \widehat{\mathcal{M}}^\dagger \widehat{\mathcal{M}}^\dagger(I) \rangle_s = \text{Cov}_{\rho_\beta}(\mathcal{M}).$$

We complete the proof of the Lemma by using Cauchy-Schwarz inequality. ■

5.2 Mixing Time, Relaxation Time, and Autocorrelation Time

Recall that \mathcal{N} and \mathcal{M} are quantum channel satisfying *s*-detailed balance with respect to ρ_β , which \mathcal{N} represents the Gibbs sampling algorithm, and \mathcal{M} represents the measurement channel.

The **mixing time** of \mathcal{N} is defined as the number of channel applications required to drive any initial state close to the Gibbs state,

$$t_{\text{mix}}(\epsilon) := \min_{t \in \mathbb{N}} \{t \geq 0 : \|\mathcal{N}^t(\rho) - \rho_\beta\|_1 \leq \epsilon, \forall \text{ quantum state } \rho\}. \quad (30)$$

The **relaxation time** of \mathcal{N} is defined as the inverse of the spectral gap

$$t_{rel} := \frac{1}{gap(\mathcal{N})}. \quad (31)$$

The relationship between mixing times and relaxation time is given by

$$(t_{rel} - 1) \log\left(\frac{1}{\epsilon}\right) \leq t_{mix}(\epsilon) \leq t_{rel} \log\left(\frac{1}{\epsilon \sigma_{min}}\right). \quad (32)$$

where σ_{min} denotes the minimum eigenvalue of the Gibbs state, which is typically exponentially small. For completeness, we put a proof of Eq. (32) in Appendix B Lemma 18.

Autocorrelation time Recall that our trajectory-based observable estimation algorithm, Algorithm 1, consists of two stages: a *burn-in stage*, in which the chain is evolved for $T_{burn} \sim t_{mix}$ to remove dependence on the initial state and reduce bias; and a *sampling stage*, where the quantum system is approximately stationary and its trajectory is used to estimate observables. The autocorrelation time quantifies the time in the sampling stage required for two outcomes to become approximately independent, with respect to the measurement \mathcal{M} .

Assuming the quantum system is already in the Gibbs state, the normalized autocorrelation function w.r.t. \mathcal{M} is defined as

$$C_{\rho_\beta}^{\mathcal{M}}(t) := \frac{\text{Corr}_{\rho_\beta}(\mathcal{E}^t)}{\text{Var}_{\rho_\beta}(\mathcal{M})} \text{ where } \mathcal{E} = \mathcal{M}\mathcal{N}\mathcal{M}. \quad (33)$$

For a finite trajectory of length K , the (finite-size integrated) autocorrelation time is defined as

$$t_{aut,K} := \frac{1}{2} + \sum_{t=1}^K \left(1 - \frac{t}{K}\right) C_{\rho_\beta}^{\mathcal{M}}(t-1). \quad (34)$$

Note that the autocorrelation time is naturally connected to the performance of empirical average, by noticing that

$$K\text{Var}_{\rho_\beta}(\mathcal{M}) 2t_{aut,K} = K\text{Var}_{\rho_\beta}(\mathcal{M}) + 2 \sum_{t=1}^K \sum_{p=1}^{K-t} \text{Corr}_{\rho_\beta}(\mathcal{E}^{p-1}) \quad (35)$$

$$= \mathbb{E}_{\rho_\beta} \left(\sum_{t=1}^K e_t - K \mathbb{E}_{\rho_\beta}(\mathcal{M}) \right)^2, \quad (36)$$

where the last equality can be verified using Eqs. (38)–(41) in Section 5.3.

We will prove that the autocorrelation time $t_{aut,K}$ is upper bounded by the relaxation time t_{rel} up to an additional factor (depending on the measurement) and an additive constant. Note that compared to t_{rel} , for $\epsilon = 1/2$, the mixing time $t_{mix}(1/2)$ includes an additional factor $\log(\sigma_{min}^{-1})$, which is often proportional to the system size n and represents the transport time across the state space. We remark that t_{rel} only gives an upper bound for $t_{aut,K}$. In practice for observables of interest, the separation between $t_{aut,K}$ and t_{mix} could be even larger than this factor $\log(\sigma_{min}^{-1})$, as illustrated in the examples in Section 1.3.

All the following lemmas are based on the finite-size autocorrelation time. For completeness, and in accordance with the classical MCMC literature, we note that the autocorrelation time for an infinitely long trajectory is defined as

$$t_{aut,\infty} := \frac{1}{2} + \sum_{t=1}^{\infty} C_{\rho_\beta}^{\mathcal{M}}(t-1). \quad (37)$$

5.3 Stationary moment identities

Before analyzing the performance of Algorithm 1, we first record some basic identities for the random variable e_t , which represents the measurement outcome in the algorithm. We denote by $\mathbb{E}_\rho[e_t]$ the expectation of e_t when the algorithm is initialized in state ρ . Similar notation is used for $\mathbb{E}_\rho[(e_t)^2]$ and the probabilities, e.g., $\mathbb{P}_\rho(\cdot)$.

Stationary case To simplify the analysis, we temporarily assume that the initial state of the sampling stage is $\rho = \rho_\beta$. To ease the notation, denote

$$v := \mathbb{E}_{\rho_\beta}(\mathcal{M}). \quad (38)$$

Recall that the Kraus operators of \mathcal{M} is $\{O_u\}_u$. When the initial state ρ is ρ_β , one can check that

$$\mathbb{E}_{\rho_\beta}[e_t] = \sum_u u \operatorname{tr}(O_u \rho_\beta O_u^\dagger) = \mathbb{E}_{\rho_\beta}(\mathcal{M}), \quad (39)$$

$$\mathbb{E}_{\rho_\beta}[(e_t - v)^2] = \sum_u |u - \mathbb{E}_{\rho_\beta}(\mathcal{M})|^2 \operatorname{tr}(O_u \rho_\beta O_u^\dagger) = \operatorname{Var}_{\rho_\beta}(\mathcal{M}). \quad (40)$$

For any $t, p > 0$, we have

$$\mathbb{E}_{\rho_\beta}[(e_t - v)(e_{t+p} - v)] = \operatorname{Corr}_{\rho_\beta}(\mathcal{E}^{p-1}), \quad (41)$$

since

$$\mathbb{E}_{\rho_\beta}[(e_t - v)(e_{t+p} - v)] = \sum_{xy} (x - v)(y - v) \operatorname{tr}(O_y(\mathcal{E}^{p-1} \circ \mathcal{M} \circ \mathcal{N}(O_x \rho_\beta O_x^\dagger)) O_y^\dagger) \quad (42)$$

$$= \sum_{xy} (x - v)(y - v) \operatorname{tr}(\mathcal{M} \circ \mathcal{N}(O_y(\mathcal{E}^{p-1} \circ \mathcal{M} \circ \mathcal{N}(O_x \rho_\beta O_x^\dagger)) O_y^\dagger)) \quad (43)$$

$$= \operatorname{tr}(\widehat{\mathcal{E}} \circ \mathcal{E}^{p-1} \circ \widehat{\mathcal{E}}(\rho_\beta)), \quad (44)$$

where Eq. (43) comes from the fact that $\mathcal{M} \circ \mathcal{N}$ is a quantum channel thus trace preserving.

5.4 Reduction from arbitrary initialization

Now we consider the case where the algorithm is initialized in an arbitrary state and a burn-in stage is used to reduce bias.

Denote $\rho_{burn} := \mathcal{N}^{T_{burn}}(\rho)$ as the state after the burn-in period.

Lemma 8 Consider quantum channels \mathcal{N} and \mathcal{M} that satisfy the s -detailed balance. Let e_t be the measurement outcome in Algorithm 1 w.r.t an arbitrary initial state ρ . For any $\epsilon, \eta > 0$, set $T_{burn} = t_{mix}(\eta)$ and

$$K \geq \frac{2\operatorname{Var}_{\rho_\beta}(\mathcal{M})}{\epsilon^2 \eta} t_{aut,K}. \quad (45)$$

We have that

$$\mathbb{P}_{\rho} \left(\left| \frac{1}{K} \left(\sum_{t=1}^K e_t \right) - \mathbb{E}_{\rho_\beta}(\mathcal{M}) \right| \geq \epsilon \right) \leq 2\eta. \quad (46)$$

Proof: First, we show that one can assume the initial state is ρ_β , at the cost of an additional error η in the probability.

Specifically, we treat all measurements performed after the burn-in period, together with the intermediate Gibbs sampling channels, as a single composite measurement. The composite measurement outcome is then $\vec{e} := (e_1, \dots, e_K) \in \mathbb{R}^K$, where we denote the associated Kraus operator as $Q_{\vec{e}}$. Denote S as the set of \vec{e} where the random variable $X_K = (e_1 + \dots + e_K)/K$ satisfies $|X_K - \mathbb{E}_{\rho_\beta}(\mathcal{M})| \geq \epsilon$. Note that

$$|\mathbb{P}_{\rho}(\vec{e} \in S) - \mathbb{P}_{\rho_\beta}(\vec{e} \in S)| = \left| \sum_{\vec{e} \in S} \operatorname{tr}(Q_{\vec{e}}(\rho_{burn} - \rho_\beta) Q_{\vec{e}}^\dagger) \right| \leq \|\rho_{burn} - \rho_\beta\|_1 \leq \eta. \quad (47)$$

Thus it suffices to assume that the initial state is ρ_β and change the error probability from 2η to η , that is, prove that

$$\mathbb{P}_{\rho_\beta} \left(\left| \frac{1}{K} \left(\sum_{t=1}^K e_t \right) - \mathbb{E}_{\rho_\beta}(\mathcal{M}) \right| \geq \epsilon \right) \leq \eta. \quad (48)$$

which follows directly from Chebyshev inequality and the formulas in the ideal case, i.e. Eqs. (39)(40)(41). ■

5.5 Time average behavior of the empirical average

Our main result is to bound the autocorrelation time $t_{aut,K}$ by the inverse spectral gap of the original quantum Gibbs sampling channel \mathcal{N} , up to an additional factor.

Lemma 9 *Let \mathcal{N} and \mathcal{M} be quantum channels satisfying Assumption 1. Suppose the map $\widehat{\mathcal{M}}$ also satisfies s -detailed balance. Then the autocorrelation time is bounded by*

$$t_{aut,K} \leq \frac{1}{\text{gap}(\mathcal{N})} \theta + \frac{1}{2}, \text{ where } \theta := \frac{\mathbb{C}\text{ov}_{\rho_\beta}(\mathcal{M})}{\mathbb{V}\text{ar}_{\rho_\beta}(\mathcal{M})}. \quad (49)$$

The proof of Lemma 9 is deferred to Section 5.6.

Together with Lemma 8 and Lemma 9, we get the theorem for the performance of the empirical averages.

Theorem 2 (Time averages) *Let \mathcal{N} and \mathcal{M} be quantum channels satisfying Assumption 1. Suppose the map $\widehat{\mathcal{M}}$ also satisfies s -detailed balance. Let e_j be the measurement outcome in Algorithm 1 w.r.t an arbitrary initial state ρ . For any $\epsilon, \eta > 0$, set $T_{burn} := t_{mix}(\eta)$ and*

$$K \geq \frac{2\mathbb{V}\text{ar}_{\rho_\beta}(\mathcal{M})}{\epsilon^2 \eta} \left(\frac{1}{\text{gap}(\mathcal{N})} \theta + \frac{1}{2} \right) \text{ for } \theta = \frac{\mathbb{C}\text{ov}_{\rho_\beta}(\mathcal{M})}{\mathbb{V}\text{ar}_{\rho_\beta}(\mathcal{M})}. \quad (50)$$

We have that

$$\mathbb{P}_\rho \left(\left| \frac{1}{K} \left(\sum_{t=1}^K e_t \right) - \mathbb{E}_{\rho_\beta}(\mathcal{M}) \right| \geq \epsilon \right) \leq 2\eta. \quad (51)$$

Remark 1 *For observables that commute with H , we construct \mathcal{M} where $\theta \leq 1$. Details are presented later in Theorem 5 in Section 6.1. We remark that the measurement cost can be reduced by skipping measurements. Let $c_{\mathcal{N}}$ and $c_{\mathcal{M}}$ denote the costs of running quantum channels \mathcal{N} and \mathcal{M} , respectively. In the above theorem, the total cost of Algorithm 1 is the sum of the following components:*

$$\text{cost of Gibbs sampling evolution} \propto t_{mix}(\eta) + \frac{1}{\text{gap}(\mathcal{N}) \epsilon^2 \eta} (c_{\mathcal{N}} \mathbb{V}\text{ar}_{\rho_\beta}(\mathcal{M})), \quad (52)$$

$$\text{cost of measurement} \propto \frac{1}{\text{gap}(\mathcal{N}) \epsilon^2 \eta} (c_{\mathcal{M}} \mathbb{V}\text{ar}_{\rho_\beta}(\mathcal{M})). \quad (53)$$

To ease notation, denote $\Delta := \text{gap}(\mathcal{N})$. Let $r := \lceil 1/\Delta \rceil$. Note that the spectral gap of \mathcal{N}^r is

$$\text{gap}(\mathcal{N}^r) = 1 - (1 - \Delta)^r \geq 1 - e^{-r\Delta} \geq 1 - e^{-1}.$$

When Δ is small and the measurement cost $c_{\mathcal{M}}$ is high, the total measurement cost can be reduced by skipping measurements. That is, one can replace \mathcal{N} with \mathcal{N}^r , or equivalently, apply the measurement \mathcal{M} every r time evolutions of \mathcal{N} instead of after every evolution. Note that the cost of total Gibbs sampling evolution in Eq. (52) remains of the same order, since by $\text{gap}(\mathcal{N}^r) \geq 1 - e^{-1}$ we have that

$$\frac{c_{\mathcal{N}}}{\text{gap}(\mathcal{N})} \sim \frac{c_{\mathcal{N}^r}}{\text{gap}(\mathcal{N}^r)}.$$

5.6 Bounding autocorrelation time by the reciprocal spectral gap

In this section we prove Lemma 9. Recall that to ease notations we write

$$v = \mathbb{E}_{\rho_\beta}(\mathcal{M}).$$

Recall that Y_i, λ_i are eigenvector and eigenvalues w.r.t. the map \mathcal{E}^\dagger . We begin by relating the correlations of the measurement outcomes to these eigenvalues.

Lemma 10 *Let \mathcal{N} and \mathcal{M} be quantum channels satisfying Assumption 1. For any integer $t, p > 0$, we have that*

$$\mathbb{E}_{\rho_\beta} [(e_t - v)(e_{t+p} - v)] = \sum_{j \geq 2} \alpha_{1j} \alpha_{j1} \lambda_j^{p-1}. \quad (54)$$

Proof: Recall that $Y_1 = I$. From Eq. (41) and Eq. (23) we have that

$$\mathbb{E}_{\rho_\beta} [(e_t - v)(e_{t+p} - v)] = \text{tr} \left(\widehat{\mathcal{E}} \circ \mathcal{E}^{p-1} \circ \widehat{\mathcal{E}} (\rho_\beta) \right) \quad (55)$$

$$= \text{tr} \left(\left(\widehat{\mathcal{E}}^\dagger (\mathcal{E}^{p-1})^\dagger \widehat{\mathcal{E}}^\dagger \right) [I] \rho_\beta \right) \quad (56)$$

$$= \sum_j \alpha_{1j} \lambda_j^{p-1} \sum_l \alpha_{jl} \langle Y_l, Y_1 \rangle_s \quad (57)$$

$$= \sum_j \alpha_{1j} \alpha_{j1} \lambda_j^{p-1}, \quad (58)$$

where we use the property that $\langle Y_l, Y_1 \rangle_s = \delta_{l1}$. Thus we complete the proof by recalling that $\alpha_{11} = 0$ [Lemma 5]. \blacksquare

Lemma 11 *Let \mathcal{N} and \mathcal{M} be quantum channels satisfying Assumption 1. We have that*

$$\mathbb{E}_{\rho_\beta} \left[\left(\sum_{t=1}^K e_t - Kv \right)^2 \right] \leq K \left(\text{Var}_{\rho_\beta}(\mathcal{M}) + \frac{2}{\text{gap}(\mathcal{N})} \mathbb{W}_{\rho_\beta}(\mathcal{E}) \right). \quad (59)$$

Proof: By Lemma 10, we have that

$$\mathbb{E}_{\rho_\beta} \left[\left(\sum_{t=1}^K e_t - Kv \right)^2 \right] = \sum_{t=1}^K \mathbb{E}_{\rho_\beta} [(e_t - v)^2] + \sum_{t=1}^K \sum_{p=1}^{K-t} 2 \mathbb{E}_{\rho_\beta} [(e_t - v)(e_{t+p} - v)] \quad (60)$$

$$= K \text{Var}_{\rho_\beta}(\mathcal{M}) + \sum_{t=1}^K \sum_{p=1}^{K-t} \sum_{j \geq 2} 2 \alpha_{1j} \alpha_{j1} \lambda_j^{p-1} \quad (61)$$

$$\leq K \text{Var}_{\rho_\beta}(\mathcal{M}) + \sum_{t=1}^K \sum_{p=1}^{K-t} \sum_{j \geq 2} 2 |\alpha_{1j} \alpha_{j1}| \lambda_j^{p-1}. \quad (62)$$

Note that by Assumption 1 and Lemma 2, we have that \mathcal{E} also has ρ_β as unique fixed state and its the spectrum is contained in $[0, 1]$. By Fact 1, we know the spectrum of \mathcal{E}^\dagger equals to the spectrum of \mathcal{E} and $\text{gap}(\mathcal{E}) = \text{gap}(\mathcal{E}^\dagger)$. Besides, from Lemma 3 we know $\text{gap}(\mathcal{E}) \geq \text{gap}(\mathcal{N})$. Thus for any $j \geq 2$, we have $\lambda_j \in [0, 1 - \text{gap}(\mathcal{N})]$.

Thus for any $j \geq 2$, one can check that

$$\sum_{t=1}^K \sum_{p=1}^{K-t} 2 \lambda_j^{p-1} = 2 \sum_{p=0}^{K-2} (K-p-1) \lambda_j^p \quad (63)$$

$$\leq 2K \sum_{p=0}^{\infty} \lambda_j^p = \frac{2K}{1 - \lambda_j} \quad (64)$$

$$\leq \frac{2K}{\text{gap}(\mathcal{N})}. \quad (65)$$

Since $\alpha_{11} = 0$ by Lemma 5, we have that the spectral covariance weight

$$\mathbb{W}_{\rho_\beta}(\mathcal{E}) := \sum_j |\alpha_{1j} \alpha_{j1}| = \sum_{j \geq 2} |\alpha_{1j} \alpha_{j1}|. \quad (66)$$

Then Eq. (62) implies

$$\mathbb{E}_{\rho_\beta} \left[\left(\sum_{t=1}^K e_t - Kv \right)^2 \right] \leq K \text{Var}_{\rho_\beta}(\mathcal{M}) + \sum_{j \geq 2} |\alpha_{1j} \alpha_{j1}| \frac{2K}{\text{gap}(\mathcal{N})} \quad (67)$$

$$= K \text{Var}_{\rho_\beta}(\mathcal{M}) + \frac{2K}{\text{gap}(\mathcal{N})} \mathbb{W}_{\rho_\beta}(\mathcal{E}). \quad (68)$$

Now finally we are prepared to prove Lemma 9, which is to bound the autocorrelation time. ■

Proof:[of Lemma 9] It suffices to notice that

$$K\mathbb{V}\text{ar}_{\rho_\beta}(\mathcal{M}) 2t_{aut,K} = K\mathbb{V}\text{ar}_{\rho_\beta}(\mathcal{M}) + 2 \sum_{t=1}^K \sum_{p=1}^{K-t} \mathbb{C}\text{orr}_{\rho_\beta}(\mathcal{E}^{p-1}) \quad (69)$$

$$= \mathbb{E}_{\rho_\beta} \left(\sum_{t=1}^K e_t - Kv \right)^2. \quad (70)$$

Then Lemma 9 follows from Lemma 11 and Lemma 7. ■

6 Implementation of the measurement

In this section, we describe the implementation of the measurement \mathcal{M} in Algorithm 1.

Structure of the section. In Section 6.1, we review Gaussian-filtered quantum phase estimation (GQPE) [24] and adapt it to our setting. For observables that commute with H , Section 6.2 uses GQPE to construct a measurement that is unbiased and satisfies detailed balance, where Theorem 2 applies directly. For concreteness, in Section 6.3, we will focus on estimating the average energy of a Gibbs state and provide a detailed comparison of the costs associated with different ways of measuring the energy. Finally, in Section 6.4, for observables that do not commute with H , we combine GQPE with an operator Fourier transform technique to construct a measurement that approximately fixes ρ_β and may mitigate disturbances from measuring general observables.

6.1 Gaussian-filtered quantum phase estimation (GQPE) and resource estimation

In this section, we review Gaussian-filtered quantum phase estimation (GQPE) [24] and adapt it to our setting. We provide a rigorous resource analysis of GQPE in Appendix D, which to our knowledge, is not available in prior literature and may be of independent interest.

Idealized Gaussian filtered quantum phase estimation To build intuition, here we describe the idealized setting, assuming that the ancillary quantum system takes continuous values. The discretization will be discussed later.

The idealized Gaussian Filtered quantum phase estimation w.r.t. observable O and parameter γ is defined w.r.t. Kraus operator

$$O_{w*} := \frac{1}{\sqrt{\gamma\sqrt{2\pi}}} \exp \left[-\frac{(w-O)^2}{4\gamma^2} \right]. \quad (71)$$

Here the subscript $*$ indicates the idealized case. In other words, the quantum channel \mathcal{M}_* is defined as

$$\mathcal{M}_*(\rho) := \int_{-\infty}^{+\infty} dw \frac{1}{\gamma\sqrt{2\pi}} \exp \left[-\frac{(w-O)^2}{4\gamma^2} \right] \rho \exp \left[-\frac{(w-O)^2}{4\gamma^2} \right]. \quad (72)$$

One can check that $\int_{-\infty}^{+\infty} O_{w*}^\dagger O_{w*} = I$ thus \mathcal{M}_* defines a quantum channel.

The first property of \mathcal{M}_* is that the measurement value with respect to the observable O can be recovered from the measurement outcome of \mathcal{M}_* : Note that $\int_w w O_{w*} O_{w*}^\dagger = O$, thus for any quantum state ρ , we have that

$$\mathbb{E}_\rho(\mathcal{M}_*) = \text{tr}(O\rho).$$

The second property is that \mathcal{M}_* inherits the commutativity property between O and ρ . First note that if O commutes with ρ , we have that $\mathcal{M}_*(\rho) = \rho$, since O_{w*} commutes with ρ and $O_{w*} = O_{w*}^\dagger$. Additionally, if the reference state ρ commutes with O , then both \mathcal{M}_* and $\widehat{\mathcal{M}}_*$ satisfy s -detailed balance with respect to ρ .

Resource estimation and properties of GQPE As in [24], the idealized Gaussian-filtered quantum phase estimation can be discretized and implemented on qubit-based quantum computers. In Appendix D, we provide a detailed discretization scheme, summarized in Algorithm 2, and a rigorous resource analysis based on the Poisson summation formula, which yields a rapidly convergent Riemann sum approximation.

With the parameter choices specified in Appendix D, for any observable O , we use GQPE to construct a measurement \mathcal{M} that has low implementation cost, enables recovery of the measurement value of O , and preserves quantitative commutativity between O and the input state. More specifically, we show that

Theorem 3 (Gaussian-filtered quantum phase estimation (GQPE)) *Let O be an observable where $\|O\| \leq \kappa = \text{poly}(n)$. Let $\epsilon > 0$ be the precision parameter. One can implement a quantum channel \mathcal{M} where for any quantum state ρ :*

- **Implementation cost:** *the measurement channel \mathcal{M} can be implemented using m ancilla qubits, t -time controlled Hamiltonian evolution of the operator O , and an additional $\text{poly}(m)$ elementary gates, such that*

$$m = \mathcal{O}(\log(\kappa) + \log \log(\epsilon^{-1})) ; \quad t = \mathcal{O}(\log(\kappa) + \log(\epsilon^{-1})).$$

- **Expectation and Variance:** *The measurement statistics can be used to recover the measurement value of O . More specifically,*

$$\begin{aligned} |\mathbb{E}_\rho[\mathcal{M}] - \text{tr}[\rho O]| &\leq \epsilon, \\ |\text{Var}_\rho[\mathcal{M}] - \text{Var}_\rho[O]| &= \mathcal{O}(1), \\ |\text{Cov}_\rho(\mathcal{M})| &\leq \text{Var}_\rho[\mathcal{M}], \end{aligned}$$

where $\text{Var}_\rho[O] := \text{tr}[O^2 \rho] - (\text{tr}[O \rho])^2$.

- **Commutativity property:** *If further $\|O\| \leq 1$, then the quantum channel \mathcal{M} approximately fixes ρ when O and ρ approximately commute, in the sense that*

$$\|\mathcal{M}[\rho] - \rho\|_1 \leq \epsilon^{-1} \text{poly} \log(\epsilon^{-1}) \| [O, \rho] \|_1 + 5\epsilon. \quad (73)$$

It is worth noting that in the implementation cost, the number of ancilla qubits and Hamiltonian evolution time all scale only polylogarithmically with the relevant parameters.

Here we remark on the ϵ^{-1} factor in Eq. (73), which reflects a tradeoff between precision and the ability to inherit the commutativity property between O and ρ . As $\epsilon \rightarrow 0$, the implemented quantum channel \mathcal{M} approaches the projective measurement of O . It is worth noting that projective measurement may not preserve the commutativity property, since eigenvectors can be highly sensitive to small perturbations. For example, a single-qubit state $\rho_\beta = |0\rangle\langle 0|$ and operator $O = I + 2^{-10}X$ have a small commutator norm, yet a projective measurement of O maps ρ to the maximally mixed state, significantly disturbing the measured state. Here Eq. (73) will be used in Section 6.4 to ensure that GQPE inherits the commutativity property when the operator Fourier transform is applied to mitigate measurement-induced disturbance.

When O and ρ exactly commute, we especially have that

Theorem 4 (Detailed Balance) *Let $\rho := \exp(-\beta H)/Z_\beta$ be the Gibbs states w.r.t. Hamiltonian H and inverse temperature β . If $[H, O] = 0$, then the GQPE measurement channel \mathcal{M} and the corresponding $\widehat{\mathcal{M}}$ satisfy the s -detailed balance w.r.t. ρ_β for any $0 \leq s \leq 1$.*

Proof: Theorem 4 directly follows from Appendix D Lemma 24 and the definition of s -detailed balance. ■

6.2 Detailed balanced measurement for commuting observables with low cost

Consider any observable O that commutes with H , such as $O = H^k$ for the integer k . Observables that commute with H correspond to the conserved quantities of a system and play a fundamental

role in understanding its thermodynamic properties. For example, $\text{tr}(H\rho_\beta)$ gives the internal energy. Together with $\text{tr}(H^2\rho_\beta)$, another observable commuting with H , allows one to determine the heat capacity. Moreover, using a telescoping technique [28], one can estimate the partition function from the ability to estimate $\text{tr}(H\rho_\beta)$ for various H . The partition function plays a central role in statistical physics, as it determines all other thermodynamic quantities, including free energy, entropy, and pressure.

As a corollary of the properties of Theorem 3 and Theorem 4 we have that

Theorem 5 (Measurement for commuting observables) *Let O be an observable that commutes with H and satisfies $\|O\| \leq \kappa = \text{poly}(n)$. Let $\epsilon > 0$ be the precision parameter. The quantum channel \mathcal{M} implemented by Algorithm 2 w.r.t. observable O satisfies that*

- **Implementation cost:** m ancilla qubits, t -time controlled Hamiltonian evolution of the operator O , an additional $\text{poly}(m)$ elementary gates, for

$$m = \mathcal{O}(\log(\kappa) + \log \log(\epsilon^{-1})) ; \quad t = \mathcal{O}(\log(\kappa) + \log(\epsilon^{-1})).$$

- **Expectation and Variance:** The measurement statistics of \mathcal{M} satisfy

$$\begin{aligned} |\mathbb{E}_{\rho_\beta}[\mathcal{M}] - \text{tr}[\rho_\beta O]| &\leq \epsilon, \\ |\text{Var}_{\rho_\beta}[\mathcal{M}] - \text{Var}_{\rho_\beta}[O]| &= \mathcal{O}(1), \\ |\mathbb{C}\text{ov}_{\rho_\beta}(\mathcal{M})| &\leq \text{Var}_{\rho_\beta}(\mathcal{M}), \end{aligned}$$

where $\text{Var}_{\rho_\beta}[O] := \text{tr}[O^2\rho_\beta] - (\text{tr}[O\rho_\beta])^2$.

- **Fixed Point and Detailed balance** The measurement \mathcal{M} fixes the Gibbs states, i.e. $\mathcal{M}(\rho_\beta) = \rho_\beta$. Both \mathcal{M} and the corresponding $\widehat{\mathcal{M}}$ satisfy the s -detailed balance w.r.t. ρ_β for any $0 \leq s \leq 1$.

To achieve an implementation cost that scales logarithmically with the precision, one may instantiate the t -time controlled Hamiltonian evolution using Hamiltonian simulation techniques with logarithmic precision dependence, such as linear-combination-of-unitaries methods [29, 30] or qubitization [31]. For geometrically local Hamiltonians, the underlying structure allows the Hamiltonian simulation to be parallelized, further reducing the circuit depth [32].

Combining Theorem 5 with Theorem 2, we obtain Corollary 12, which applies to any observable O that commutes with H . As an example, in Section 6.3 we focus on the case $O = H$ and compare the gate and depth complexity of GQPE with those of other approaches for estimating the same observable.

Corollary 12 (Thermal expectation estimation for commuting observables) *Let \mathcal{N} be a Gibbs sampling algorithm that satisfies s -detailed balance with respect to the Gibbs state $\rho_\beta = e^{-\beta H}/Z_\beta$, has ρ_β as its unique fixed point, and has a spectrum in $[0, 1]$. For any observable O commuting with H and obeying $\|O\| \leq \kappa = \text{poly}(n)$, one can estimate $\text{tr}(O\rho_\beta)$ to precision ϵ with probability at least $1 - 2\eta$ using m ancilla qubits, $t_{\mathcal{N}}$ -time of \mathcal{N} , and $t_{\mathcal{M}}$ -time of controlled Hamiltonian evolution of O , where*

$$m = \mathcal{O}(\log \kappa + \log \log \epsilon^{-1}), \quad t_{\mathcal{N}} = t_{\text{mix}} + \mathcal{O}\left(\frac{\text{Var}_{\rho_\beta}[O]}{\epsilon^2 \eta \text{gap}(\mathcal{N})}\right), \quad t_{\mathcal{M}} = \tilde{\mathcal{O}}\left(\frac{\text{Var}_{\rho_\beta}[O]}{\epsilon^2 \eta \text{gap}(\mathcal{N})}\right)$$

where $\tilde{\mathcal{O}}(\cdot)$ hides a factor of $\text{polylog}(\epsilon^{-1}) + \text{polylog}(\kappa)$. The cost $t_{\mathcal{M}}$ can be reduced by a factor of $\text{gap}(\mathcal{N})^{-1}$, that is, to $\tilde{\mathcal{O}}(\text{Var}_{\rho_\beta}[O]/(\epsilon^2 \eta))$ by skipping measurement, as noted in Remark 1.

6.3 Energy function estimation and cost comparison

In this section, we illustrate the effectiveness of Theorem 3 by analyzing a concrete example. In particular, here we focus on the case where $O = H$ and set the goal as estimating $\text{tr}(H\rho_\beta)$ to precision ϵ . Here for simplicity we also assume that H is defined on a 2D lattice to enable a meaningful comparison of circuit depth.

To begin with, we clarify the key quantities that will be compared. Suppose \mathcal{M} is a quantum channel that implements a measurement of H , in the sense that its output expectation value equals

$\text{tr}(H\rho_\beta)$. Let $c_{\mathcal{M}}$ and $d_{\mathcal{M}}$ denote, respectively, the gate cost and depth cost of performing a single use of \mathcal{M} .

According to Theorem 2 and Remark 1, Eqs. (52)(53), the dominant factors of the total cost are the measurement variance $\text{var}_{\mathcal{M}} := \text{Var}_{\rho_\beta}(\mathcal{M})$, which determines the total cost of the Gibbs-sampling evolution, and the product $c_{\mathcal{M}} \times \text{var}_{\mathcal{M}}$, which determines the total gate cost of implementing the measurement. Similarly, we also consider the product $d_{\mathcal{M}} \times \text{var}_{\mathcal{M}}$, which determines the total circuit depth incurred by the measurement. In what follows, we estimate these quantities for different choices of \mathcal{M} and show that the GQPE procedure described in Theorem 3 achieves the smallest cost (up to a $\text{poly log}(\epsilon^{-1})$ factor) on all those quantities. The comparison is summarized in Table 1 in the introduction section. Note that Theorem 3 implies that for GQPE, the factor θ in Theorem 2 satisfies $\theta \leq 1$, thus we ignore this factor.

Notations and Scaling of $\mathbb{E}_{\rho_\beta}(H)$ and $\text{Var}_{\rho_\beta}(H)$ Recall that n is the number of qubits in the Hamiltonian H . We assume that H is defined on a 2D lattice, so it consists of $\mathcal{O}(n)$ local terms. The expectation value $\mathbb{E}_{\rho_\beta}(H) := \text{tr}(H\rho_\beta)$ represents the internal energy of the system, and the variance $\text{Var}_{\rho_\beta}(H) := \text{tr}(H^2\rho_\beta) - (\text{tr}(H\rho_\beta))^2$ is related to the heat capacity. For finite β , both $\mathbb{E}_{\rho_\beta}(H)$ and $\text{Var}_{\rho_\beta}(H)$ typically scale linearly with the system size, i.e., $\mathcal{O}(n)$.

Classical Hamiltonian For comparison, we also list the cost in the classical setting. First note that when H is a classical Hamiltonian, give a sample x from the Gibbs distribution, where x is a computational basis, one can compute the corresponding energy $\langle x|H|x\rangle$ to high precision (in fact exactly) in time $\mathcal{O}(n)$. Since we assume the Hamiltonian is on 2D, the computation can be parallel to depth $\mathcal{O}(1)$. The variance of $\langle x|H|x\rangle$, when consider the randomness of x , is the same as $\text{Var}_{\rho_\beta}(H)$ which scales as $\mathcal{O}(n)$.

High precision (HP) QPE When H is a quantum Hamiltonian, to perform a high precision energy estimation, i.e. to precision ϵ , quantum phase estimation algorithm has a gate cost as $\Omega(n\epsilon^{-1})$, and a depth cost as $\Omega(\epsilon^{-1})$ [see survey [21] and [23]]. The variance of this measurement is of the same order as $\text{Var}_{\rho_\beta}(H)$ which scales as $\mathcal{O}(n)$.

Local Measurement Another simple way to measure $H = \sum_{i=1}^{\kappa} H_i$ is to randomly measure its local terms. Given an input state ρ_β , one can randomly select a local term H_i according to a uniform distribution and perform a projective measurement with respect to H_i on ρ_β . Denote the measurement outcome as Y_i and set the energy estimate $X_i := \kappa Y_i$. One can check that $E(X_i) = \text{tr}(H\rho_\beta)$.

Since this measurement only measures a single local term at a time, we have $c_{\mathcal{M}} = \mathcal{O}(1)$. However, it increases the variance by a factor of $\mathcal{O}(n)$ compared to $\text{Var}_{\rho_\beta}(H)$, as

$$\text{var}(X_i) = \kappa \text{tr} \left(\sum_i H_i^2 \rho_\beta \right) - \text{tr}^2(H\rho_\beta) = \mathcal{O}(\kappa^2) = \mathcal{O}(n^2).$$

Another drawback of this randomized local measurement is that it is incoherent (destructive) and substantially disturbs the Gibbs state. A potential remedy is to apply a recovery channel after the destructive measurement: using the quantum Markov property, in the geometrically local case, a quasi-local recovery map can drive the perturbed state back to the Gibbs state [33], at a cost that grows polynomially with ϵ^{-1} and β . Analyzing the correlation between samples in this approach is beyond the scope of this manuscript and is left as an open question.

GQPE For GQPE, with the parameters choices in Algorithm 2, according to Theorem 3 we know the cost of implementing a single \mathcal{M} is dominated by implementing the controlled Hamiltonian evolution

$$W = \sum_{\ell=0}^{N-1} e^{-2\pi i \xi_\ell H/\kappa} \otimes |\ell\rangle\langle\ell| = e^{\pi i N h H/\kappa} \sum_{\ell=0}^{N-1} e^{-2\pi i \ell h H/\kappa} \otimes |\ell\rangle\langle\ell|, \quad (74)$$

where the maximal simulation time of H is $t_{\max} \leq 2\pi N h/\kappa \leq \mathcal{O}(\log(n\epsilon^{-1}))$. By [32], for a simulation time $0 \leq t \leq t_{\max}$, the time-evolution operator e^{-itH} can be implemented up to precision ϵ using $\mathcal{O}(n \text{poly log}(n\epsilon^{-1}))$ gates and $\mathcal{O}(\text{poly log}(n\epsilon^{-1}))$ depth. Then, using a standard technique

for controlled Hamiltonian simulation [34, Lemma 8], the controlled Hamiltonian evolution W in Eq. (74) can be constructed using $\mathcal{O}(n \text{poly log}(n\epsilon^{-1}))$ elementary gates and circuit depth, with an additional $\mathcal{O}(\log(n))$ ancilla qubits. Note that the circuit depth of the controlled unitary can be further reduced to $\mathcal{O}(\text{poly log}(n\epsilon^{-1}))$ circuit depth by introducing $\mathcal{O}(n \text{poly log}(n\epsilon^{-1}))$ copies of classical control bits, similar to techniques used in [35].

6.4 Mitigating Measurement Disturbance for non-commuting observable via Operator Fourier Transform

From the previous sections, particularly Theorems 2 and Theorem 5, we see that for observables commuting with H , *effectively* independent samples can be obtained on a timescale shorter than the mixing time. One intuitive reason for this Gibbs sampling reduction is that the GQPE measurement leaves the Gibbs state invariant, so no additional burn-in period is required after the measurement.

In this section, we consider measuring a local observable O that does not commute with H . A direct projective measurement of such an observable would significantly disturb the Gibbs state and introduce bias. Guided by the intuition discussed above, here we investigate an operator Fourier transform technique [25] to construct a measurement that approximately preserves the Gibbs state.

We remark that Theorem 2 does not directly apply to the measurement constructed in this section, since it does not satisfy *exact* detailed balance, although it approximately preserves the Gibbs state. We leave addressing this gap to future work.

Weighted Operator Fourier Transform (WOFT) [25] First we explain the weighted operator Fourier transform and the key observations. Recall that H is a local Hamiltonian and $\rho_\beta = \exp(-\beta H)/Z_\beta$ is the Gibbs state at inverse temperature β .

Consider the spectrum decomposition of H , that is, $H := \sum_k E_k \Pi_k$, where E_k is the eigenvalue and Π_k is the corresponding spectral projector. To ease notations, define the set of spectrum as $\text{Spec}(H) := \{E_k\}_k$ and define the set of energy difference, namely Bohr frequency, as

$$\text{Bohr}(H) := \{E_i - E_j \mid E_i, E_j \in \text{Spec}(H)\}. \quad (75)$$

The Fourier components of O w.r.t. frequency ν is defined as

$$O_\nu := \sum_{i,j: E_i - E_j = \nu} \Pi_i O \Pi_j. \quad (76)$$

Definition 13 (Weighted Operator Fourier Transform (WOFT) [25]) Given an observable O with $\|O\| \leq 1$, a reference Hamiltonian H , a function $f(t) = \frac{\tau}{\sqrt{\pi}} e^{-\tau^2 t^2}$ with parameter τ , the weighted operator Fourier transform is defined as

$$\widehat{O}(\tau) := \int_{-\infty}^{+\infty} e^{iHt} O e^{-iHt} f(t) dt = \sum_{\nu \in \text{Bohr}(H)} \exp\left(-\frac{\nu^2}{4\tau^2}\right) O_\nu. \quad (77)$$

The key observation is as follows:

Observation 1 For any observable O , define $\widehat{O}(\tau)$ as in Eq. (77). Then the following holds:

- **Observable value:** The WOFT does not change the observable value. That is, for any τ ,

$$\text{tr}(\rho_\beta \widehat{O}(\tau)) = \text{tr}(\rho_\beta O_0) = \text{tr}(\rho_\beta O).$$

- **Decay of Commutator norm:** WOFT filters out the components that do not commute with H . From Eq. (77), as $\tau \rightarrow 0$, $\widehat{O}(\tau)$ converges to O_0 that commutes with H . Consequently,

$$\left\| [\widehat{O}(\tau), \rho_\beta] \right\|_1 \rightarrow 0 \quad \text{as } \tau \rightarrow 0.$$

- **Norm bound:** Note that WOFT does not increase the spectrum norm, that is,

$$\|\widehat{O}(\tau)\| \leq \int_{-\infty}^{+\infty} \|e^{iHt} O e^{-iHt}\| f(t) dt = 1.$$

Mitigate measurement disturbance by WOFT In this section, we consider a local observable O satisfying $\|O\| \leq 1$. Observation 1 shows that, to estimate $\text{tr}(O\rho_\beta)$, one may instead measure the Fourier-transformed operator $\widehat{O}(\tau)$, since it has the same expectation value. Moreover, measuring $\widehat{O}(\tau)$ for small τ is expected to introduce less disturbance to the Gibbs state, since $\|[\widehat{O}(\tau), \rho_\beta]\|_1$ becomes small when τ is small. The measurement for the Fourier-transformed operator $\widehat{O}(\tau)$ can be implemented by GQPE combined with standard Hamiltonian simulation techniques like linear combination of unitaries. More specifically,

Theorem 6 (Measurement for non-commuting observables) *Consider any local observable O such that $\|O\| \leq 1$. Let ϵ be a precision parameter. Set τ small enough such that $\|[\widehat{O}(\tau), \rho_\beta]\|_1 \leq \epsilon^2$. Then the quantum channel \mathcal{M} implemented by Algorithm 2 w.r.t. discretized version of observable $\widehat{O}(\tau)$ satisfies that*

- **Expectation and Variance:** The measurement statistics of \mathcal{M} satisfy

$$\begin{aligned} |\mathbb{E}_{\rho_\beta}[\mathcal{M}] - \text{tr}[\rho_\beta O]| &\leq 2\epsilon, \\ |\text{Var}_{\rho_\beta}[\mathcal{M}] - \text{Var}_{\rho_\beta}[O]| &= \mathcal{O}(1), \\ |\text{Cov}_{\rho_\beta}(\mathcal{M})| &\leq \text{Var}_{\rho_\beta}[\mathcal{M}], \end{aligned}$$

where $\text{Var}_{\rho_\beta}[O] := \text{tr}[O^2 \rho_\beta] - (\text{tr}[O \rho_\beta])^2$.

- **Approximate fixed point** The measurement \mathcal{M} approximately fixed the Gibbs state,

$$\|\mathcal{M}[\rho_\beta] - \rho_\beta\|_1 \leq \epsilon \text{poly log}(\epsilon^{-1}) + 5\epsilon.$$

- **Implementation cost:** m ancilla qubits, t -time controlled Hamiltonian evolution of H , and $\text{poly log}(\tau^{-1} \epsilon^{-1} \|H\|)$ additional elementary gates, for

$$m = \mathcal{O}(\log(\tau^{-1} \epsilon^{-1} \|H\|)), \quad t = \mathcal{O}(\tau^{-1} \text{poly log}(\epsilon^{-1} \tau^{-1})) \quad (78)$$

When the commutator norm $\|[\widehat{O}(\tau), \rho_\beta]\|_1$ decays exponentially fast as $\mathcal{O}(\exp(-\mathcal{O}(1/\tau^2)))$, it suffices to choose $\tau^{-1} = \mathcal{O}(\log \epsilon^{-1})$.

If further O and H are geometrically local, the Lieb–Robinson bounds imply that the implementation cost can be reduced to: m ancilla qubits, and a t -time controlled Hamiltonian evolution of a quasi-local operator instead of the full t -time controlled Hamiltonian evolution of H . Since the number of controlled bits (i.e. m) is logarithmic, such a quasi-local evolution for time t can be implemented using $\text{poly log}(n) + \text{poly log}(\epsilon^{-1})$ elementary gates.

The proof of Theorem 6 is put into Appendix A and is mainly a corollary of Theorem 3 combined with standard technique of Hamiltonian simulation for the discretized version of $\widehat{O}(\tau)$.

According the Eq. (78), the implementation cost is mainly determined by τ^{-1} , thus determined by the commutator norm decay rate. We note that one scenario in which the commutator norm decays exponentially is that O induces a large energy disturbance, especially in the low-energy eigenspace. For example, if H is the 2D Toric code and O a single-qubit Pauli X , each eigenstate $|\psi\rangle$ of H is mapped to another state $O|\psi\rangle$ which has energy difference 2, this will implies $\|[\widehat{O}(\tau), \rho_\beta]\|_1 \leq 2 \exp(-\frac{1}{\tau^2})$. Another example arises when measuring the zero-temperature Gibbs state (i.e. ground state) of a gapped system. In particular, when $\beta = +\infty$ and the Hamiltonian has a spectral gap c between the ground-state energy and the first excited energy, then for any observable O with $\|O\| \leq 1$, one have that $\|[\widehat{O}(\tau), \rho_\beta]\|_1 \leq 2 \exp(-\frac{c^2}{4\tau^2})$. Further details on these two examples are given in Appendix C.

We remark that although Theorem 6 shows that the implemented measurement \mathcal{M} approximately fixes the Gibbs state—suggesting that an additional burn-in period may not be necessary—we cannot directly apply Lemma 9 and Theorem 2, since \mathcal{M} does not satisfy *exact* detailed balance. We leave addressing this gap to future work.

Acknowledgement

This work is partially supported by the Simons Quantum Postdoctoral Fellowship (J.J., J.L.), by a Simons Investigator Award in Mathematics through Grant No. 825053 (J.L., L.L.), and by the Challenge Institute for Quantum Computation (CIQC) funded by National Science Foundation (NSF) through grant number OMA-2016245 (L.L.). We thank Joao Basso and Sandy Irani for helpful discussions.

A Proof of Theorem 6

In this section, we give the proof for Theorem 6.

Discretization of $\hat{O}(\tau)$ First, we specify the discretization of $\hat{O}(\tau)$. Set integers

$$T = \mathcal{O}(\tau^{-1} \log(\epsilon^{-1} \tau^{-1})), \quad L = \mathcal{O}(\epsilon^{-1} \|H\| \tau^{-1}). \quad (79)$$

We truncate the infinite integral in $\hat{O}(\tau)$ to $[-T, T]$ and discretize the truncated integral with step size L^{-1} . More specifically, define the quadrature points as $t_j = -T + jL^{-1}$ for $j = 0$ to $2TL - 1$. The discretized version of $\hat{O}(\tau)$ is

$$\hat{O}_{\text{dis}}(\tau) := \sum_{j=0}^{2TL-1} \frac{1}{L} e^{iHt_j} O e^{-iHt_j} f(t_j). \quad (80)$$

Using standard analyses of integral discretization, one can verify that

$$\left\| \hat{O}(\tau) - \hat{O}_{\text{dis}}(\tau) \right\| \leq \epsilon. \quad (81)$$

Proof of Theorem 6 The measurement \mathcal{M} is implemented by Algorithm 2 with respect to the observable $\hat{O}_{\text{dis}}(\tau)$. First, note that the expectation and variance properties in Theorem 6 follow as a corollary of Theorem 3. In particular, since $\|\hat{O}_{\text{dis}}(\tau) - \hat{O}(\tau)\| \leq \epsilon$ and $\|\hat{O}(\tau)\| \leq 1$ by Observation 1, Theorem 3 guarantees that the expectation and variance bounds hold. Furthermore, the approximate fixed-point property in Theorem 6 directly follows from the commutativity property established in Theorem 3.

From Theorem 3, the implementation cost of \mathcal{M} is dominated by controlled Hamiltonian simulation for $\hat{O}_{\text{dis}}(\tau)$ for time $t = \mathcal{O}(\log \epsilon^{-1})$, which is dominated by Hamiltonian simulation for $\hat{O}_{\text{dis}}(\tau)$. In the following, we analyze the simulating $e^{it\hat{O}_{\text{dis}}(\tau)}$ by standard techniques for

$$t = \mathcal{O}(\log \epsilon^{-1}).$$

Geometrically local case We begin with the special case when both H, O are geometrically local on a D -dimensional lattice. In addition assume $\tau^{-1} = \mathcal{O}(\log \epsilon^{-1})$ thus $T = \text{poly log}(\epsilon^{-1})$.

Let Ω denote a set of qubits on the lattice whose support is slightly larger than that of O . Specifically, the distance between $\text{supp}(O)$ and any qubit outside Ω is $\mathcal{O}(\log \epsilon^{-1} + \log \|H\|)$. Since $|t_j| \leq T$ for all j , by the Lieb–Robinson bound (Lemma 5 in [32]), for any j one can approximate $e^{iHt_j} O e^{-iHt_j}$ to precision $\epsilon/(2TL)$ by an operator supported on Ω . Consequently, $\hat{O}_{\text{dis}}(\tau)$ can be approximated to precision ϵ by an operator supported on Ω , whose locality is $\mathcal{O}(\log^D(\epsilon^{-1}) + \log^D(\|H\|))$, where D is the lattice dimension. Thus, one can simulate $e^{it\hat{O}_{\text{dis}}(\tau)}$ for $t = \mathcal{O}(\log \epsilon^{-1})$ with gate complexity $\mathcal{O}(\text{poly log}(\epsilon^{-1}) \times \text{poly log}(\|H\|))$ using Hamiltonian simulation methods that achieve logarithmic dependence on the precision [29, 30, 31].

General case For general case where H, O might not be geometrically local and τ^{-1} may be large. Recall that

$$T = \mathcal{O}(\tau^{-1} \log(\epsilon^{-1} \tau^{-1})), \quad L = \mathcal{O}(\epsilon^{-1} \|H\| \tau^{-1}). \quad (82)$$

A standard approach to simulating $e^{it\hat{O}_{\text{dis}}(\tau)}$ is to use the linear combination of unitaries (LCU) technique. General references on LCU can be found in [29, 36].

Consider decomposing O into a sum of Paulis, that is,

$$O = \sum_{k=1}^{\kappa_O} u_k U_k,$$

where each U_k is a local Pauli operator (unitary and Hermitian). Since we assume that O is local and $\|O\| = \mathcal{O}(1)$, we have $\kappa_O = \mathcal{O}(1)$ and $|u_k| = \mathcal{O}(1)$. Absorbing the sign of u_k into the Pauli, we may write equivalently $O = \sum_{k=1}^{\kappa_O} a_k P_k$ with $a_k := |u_k| \geq 0$ and $P_k := \text{sgn}(u_k) U_k$. Then

$$\widehat{O}_{\text{dis}}(\tau) := \sum_{k=1}^{\kappa_O} \sum_{j=0}^{2TL-1} a_k f(t_j) \frac{1}{L} e^{iHt_j} P_k e^{-iHt_j}. \quad (83)$$

$$t_j = -T + jL^{-1}. \quad (84)$$

Set $s_1 = \mathcal{O}(1)$ to be an integer such that $2^{s_1} \geq \kappa_O$. For simplicity, we choose T, L such that $2TL = 2^{s_2}$ for some integer

$$s_2 = \mathcal{O}(\log(\tau^{-1} \epsilon^{-1} \|H\|))$$

Define R to be a $(s_1 + s_2)$ -qubit unitary that can prepare the following state,

$$R |0^{s_1}\rangle_1 |0^{s_2}\rangle_2 := \left(\frac{1}{\sqrt{C_O}} \sum_{k=1}^{\kappa_O} \sqrt{a_k} |k\rangle_1 \right) \otimes \left(\frac{1}{\sqrt{C_f}} \sum_{j=0}^{2TL-1} \frac{1}{\sqrt{L}} \sqrt{f(t_j)} |j\rangle_2 \right). \quad (85)$$

where the subscripts $|\cdot\rangle_1$ and $|\cdot\rangle_2$ refer to different registers. Note that the normalization factor $C_O := \sum_{k=1}^{\kappa_O} a_k = \mathcal{O}(1)$ since $\kappa_O = \mathcal{O}(1)$ and $a_k = \mathcal{O}(1)$. Besides, by the choice of parameters we know that C_f satisfies

$$|C_f - 1| := \left| \sum_{j=0}^{2TL-1} \frac{1}{L} f(t_j) - 1 \right| \leq \epsilon.$$

Thus the total normalization factor satisfies

$$\alpha := C_O C_f = \mathcal{O}(1). \quad (86)$$

Define an $(s_1 + s_2 + n)$ -qubit unitary (which is called the select oracle)

$$U := \sum_{k=1}^{\kappa_O} \sum_{j=0}^{2TL-1} |k\rangle_1 \langle k|_1 \otimes |j\rangle_2 \langle j|_2 \otimes e^{iHt_j} P_k e^{-iHt_j}. \quad (87)$$

Then the $(s_1 + s_2 + n)$ -qubit unitary $R^\dagger U R$ is a $(\alpha, s_1 + s_2, 0)$ -block encoding of $\widehat{O}_{\text{dis}}(\tau)$, in the sense that

$$\left\| \widehat{O}_{\text{dis}}(\tau) - \alpha \left(\langle 0^{s_1+s_2} |_{12} \otimes I | R^\dagger U R | 0^{s_1+s_2} \rangle_{12} \otimes I \right) \right\|_2 = 0. \quad (88)$$

Recall that $\alpha = \mathcal{O}(1)$. By [29, Definition 43 and Corollary 60], one can implement the Hamiltonian evolution $e^{it\widehat{O}_{\text{dis}}(\tau)}$ for $t = \mathcal{O}(\log \epsilon^{-1})$ to precision ϵ using

- $(s_1 + s_2)$ ancilla qubits, where $s_1 = \mathcal{O}(1)$ and $s_2 = \mathcal{O}(\log(\tau^{-1} \epsilon^{-1} \|H\|))$,
- $\mathcal{O}(t + \log \epsilon^{-1})$ applications of the block-encoding $R^\dagger U R$ (and its inverse). Recall in our case $t = \mathcal{O}(\log \epsilon^{-1})$.

where R can be implemented with $2^{s_1} \times \text{poly}(s_2)$ elementary gates using Gaussian state preparation algorithms such as [37], and since $|t_j| \leq T$, we have that U corresponds to performing controlled Hamiltonian evolution of H for time

$$\mathcal{O}(\tau^{-1} \log(\epsilon^{-1} \tau^{-1})).$$

B Quantum detailed balance and its property

In this section, we prove some basic properties of quantum detailed balance. We use \mathbb{M} to denote the linear space formed by all $\mathbb{C}^{2^n \times 2^n}$ matrices. Let ρ_β be the Gibbs state. For any $s \in [0, 1]$, define the linear map $\mathcal{F}_s : \mathbb{M} \rightarrow \mathbb{M}$ to be

$$\mathcal{F}_s(A) = \rho_\beta^{1-s} A \rho_\beta^s, \quad \forall A \in \mathbb{M}. \quad (89)$$

Note that ρ_β is full-rank thus \mathcal{F}_s is invertible.

For two matrices $A, B \in \mathbb{M}$, the *Hilbert-Schmidt inner product* (HS) is defined as

$$\langle A, B \rangle := \text{tr}(A^\dagger B). \quad (90)$$

The weighted inner product is defined as

$$\langle A, B \rangle_s := \langle A, \mathcal{F}_s(B) \rangle = \text{tr}(A^\dagger \rho_\beta^{1-s} B \rho_\beta^s). \quad (91)$$

One can verify that $\langle \cdot, \cdot \rangle_s$ defines a valid inner product. In particular, $\langle \cdot, \cdot \rangle_{\frac{1}{2}}$ is known as the KMS inner product. One can check that

Lemma 14 *Since ρ_β is a Hermitian operator, we have that \mathcal{F}_s is Hermitian w.r.t. HS. That is $\langle A, \mathcal{F}_s(B) \rangle = \langle \mathcal{F}_s(A), B \rangle$.*

Recall that given a linear map \mathcal{T} , the \mathcal{T}^\dagger is its dual map w.r.t. HS.

Definition 15 (Quantum detailed balance) *We say that a linear map $\mathcal{T} : \mathbb{M} \rightarrow \mathbb{M}$ satisfying the s -quantum detailed balance w.r.t. ρ_β , if \mathcal{T}^\dagger is Hermitian w.r.t. the weighted inner product $\langle \cdot, \cdot \rangle_s$, that is*

$$\langle A, \mathcal{T}^\dagger(B) \rangle_s = \langle \mathcal{T}^\dagger(A), B \rangle_s. \quad (92)$$

which is equivalent to

$$\mathcal{T} \circ \mathcal{F}_s = \mathcal{F}_s \circ \mathcal{T}^\dagger. \quad (93)$$

Note that $\mathcal{T} \circ \mathcal{F}_s = \mathcal{F}_s \circ \mathcal{T}^\dagger$ implies that

$$\mathcal{F}_s^{-1/2} \circ \mathcal{T} \circ \mathcal{F}_s^{1/2} = \mathcal{F}_s^{1/2} \circ \mathcal{T}^\dagger \circ \mathcal{F}_s^{-1/2}, \quad (94)$$

$$\mathcal{F}_s^{-1} \circ \mathcal{T} = \mathcal{T}^\dagger \circ \mathcal{F}_s^{-1}, \quad (95)$$

where Eq. (95) implies that \mathcal{T} is Hermitian w.r.t. another weighted inner product $\langle \cdot, \cdot \rangle_{*s}$,

$$\langle A, \mathcal{T}(B) \rangle_{*s} = \langle \mathcal{T}(A), B \rangle_{*s} \quad (96)$$

$$\text{for } \langle A, B \rangle_{*s} := \text{tr}(A^\dagger \rho_\beta^{s-1} B \rho_\beta^{-s}). \quad (97)$$

Lemma 16 (Properties of quantum detailed balance) *Consider a linear map $\mathcal{T} : \mathbb{M} \rightarrow \mathbb{M}$ satisfying the s -quantum detailed balance w.r.t. ρ_β . Then*

- (1) *If in addition \mathcal{T}^\dagger is unital, i.e. $\mathcal{T}^\dagger(I) = I$, then ρ_β is a fixed state of \mathcal{T} , i.e. $\mathcal{T}(\rho_\beta) = \rho_\beta$. Note that when \mathcal{T} is a quantum channel, \mathcal{T}^\dagger is unital.*
- (2) $\mathcal{F}_s^{-1/2} \circ \mathcal{T} \circ \mathcal{F}_s^{1/2}$ is Hermitian w.r.t. HS.
- (3) *The maps $\mathcal{F}_s^{-1/2} \circ \mathcal{T} \circ \mathcal{F}_s^{1/2}$, $\mathcal{F}_s^{1/2} \circ \mathcal{T}^\dagger \circ \mathcal{F}_s^{-1/2}$, \mathcal{T} and \mathcal{T}^\dagger are diagonalizable. Besides, all the four maps have the same real spectrum.*
- (4) *If \mathcal{T} is a quantum channel, then its spectrum lies in $[-1, 1]$.*
- (5) *If $\mathcal{T} = e^{t\mathcal{L}}$ for a Lindbladian \mathcal{L} and $t > 0$, and moreover $e^{t\mathcal{L}}$ satisfies the s -quantum detailed balance condition w.r.t. ρ_β , then its spectrum lies in $[0, 1]$.*

(6) When \mathcal{T} is a quantum channel and ρ_β is its unique fixed state, its spectral gap can be characterized by

$$\text{gap}(\mathcal{T}) = \text{gap}(\mathcal{T}^\dagger) = 1 - \max_{X \in \mathbb{M}, \langle X, I \rangle_s = 0} \frac{\langle X, \mathcal{T}^\dagger(X) \rangle_s}{\langle X, X \rangle_s} \quad (98)$$

Proof: (1) comes from applying both sides of Eq. (93) to I . (2) comes from the fact that \mathcal{F}_s is Hermitian w.r.t. HS and Eq. (94).

For (3), from (2) we know that $\mathcal{F}_s^{-1/2} \circ \mathcal{T} \circ \mathcal{F}_s^{1/2}$ is Hermitian w.r.t. HS, thus it is diagonalizable w.r.t. basis $\{Y_1, \dots, Y_n\} \subseteq \mathbb{M}$, and has a real spectrum,

$$\mathcal{F}_s^{-1/2} \circ \mathcal{T} \circ \mathcal{F}_s^{1/2}[Y_i] = \lambda_i Y_i, \text{ where } \lambda_i \in \mathbb{R}, \quad (99)$$

which implies that $\mathcal{F}_s^{1/2} Y_i$ is the eigenvector of \mathcal{T} w.r.t. eigenvalue λ_i . Thus \mathcal{T} is also diagonalizable and has the same spectrum. Then it suffices to recall Eq. (94) which says that

$$\mathcal{F}_s^{-1/2} \circ \mathcal{T} \circ \mathcal{F}_s^{1/2} = \mathcal{F}_s^{1/2} \circ \mathcal{T}^\dagger \circ \mathcal{F}_s^{-1/2}.$$

For (4), let $Y \in \mathbb{M}$ be an eigenvector of \mathcal{T} with eigenvalue λ . Since quantum channel does not increase the trace-norm, $|\lambda| \|Y\|_1 = \|\mathcal{T}(Y)\|_1 \leq \|Y\|_1$, which implies $\lambda \in [-1, 1]$.

For (5), let μ be an eigenvalue of \mathcal{L} . By the semigroup property, $e^{t\mu}$ is an eigenvalue of $e^{t\mathcal{L}}$ for all $t \geq 0$. By the additional assumption, each $e^{t\mathcal{L}}$ satisfies s -detailed balance, hence by (3) its spectrum is real, and by (4) it lies in $[-1, 1]$. Therefore $e^{t\mu} \in [-1, 1]$ for all $t \geq 0$, which forces $\mu \leq 0$. Hence the spectrum of $\mathcal{T} = e^{t\mathcal{L}}$ is contained in $[0, 1]$. (Here we use the fact that $e^{t\mathcal{L}}$ is a quantum channel for all $t \geq 0$; see, e.g., [38, Theorem 7.1].)

For (6), by (3) we know that \mathcal{T} and \mathcal{T}^\dagger have the same spectrum thus (i) They have the same spectral gap, (ii) \mathcal{T}^\dagger should also have unique fixed state, which is I . Then (6) comes from the fact that \mathcal{T}^\dagger is Hermitian w.r.t. $\langle \cdot, \cdot \rangle_s$, its maximum eigenvalue is 1 w.r.t. eigenstate I , and the definition of spectral gap. \blacksquare

Lemma 17 Suppose \mathcal{T} is a quantum channel that satisfies s -detailed balance w.r.t. ρ_β . Then for any operator A we have that

$$\langle A, A \rangle_{*s} \geq \langle \mathcal{T}(A), \mathcal{T}(A) \rangle_{*s}. \quad (100)$$

If further \mathcal{T} has ρ_β as its unique fixed state, the spectrum of \mathcal{T} lies in $[0, 1]$, and the operator A is non-trivial and traceless, i.e. $A \neq 0$ and $\text{tr}(A) = 0$, then we have that \mathcal{T} is strictly contractive, i.e. the \geq in Eq. (100) becomes $>$.

Proof: From Eq. (96) we know that \mathcal{T} is Hermitian w.r.t. $\langle \cdot, \cdot \rangle_{*s}$, thus there exists a set of eigenbasis $\{Z_i\}_i \subseteq \mathbb{M}$ which is orthonormal w.r.t. $\langle \cdot, \cdot \rangle_{*s}$, and satisfies $\mathcal{T}(Z_i) = \lambda_i Z_i$. From Lemma 16 (4) we know that $\lambda_i \in [-1, 1]$. Consider decomposing A onto the basis $\{Z_i\}_i$ as $A = \sum_i \alpha_i Z_i$. We have

$$\langle A, A \rangle_{*s} = \sum_i |\alpha_i|^2 \geq \sum_i \lambda_i^2 |\alpha_i|^2 = \langle \mathcal{T}(A), \mathcal{T}(A) \rangle_{*s}. \quad (101)$$

If further \mathcal{T} has ρ_β as its unique fixed state and has a spectrum in $[0, 1]$, we have that $1 = \lambda_1 > \lambda_2 \dots \geq 0$ and $Z_1 = \rho_\beta$. For the case of traceless A , it suffices to notice that $\text{tr}(A) = 0$ implies

$$\alpha_1 = \langle A, Z_1 \rangle_{*s} = \langle A, \rho_\beta \rangle_{*s} = 0,$$

Thus $\langle A, A \rangle_{*s} > \langle \mathcal{T}(A), \mathcal{T}(A) \rangle_{*s}$, since $\forall i \geq 2, |\lambda_i| < 1$ and $A \neq 0$. \blacksquare

Finally we prove Lemma 2.

Proof: [of Lemma 2] One can verify that \mathcal{MNM} satisfies s -detailed balance by directly applying the definition of detailed balance. We prove the fixed point is unique by contradiction. For any operator A , denote $\|A\|_{*s} := \sqrt{\langle A, A \rangle_{*s}}$. Note that \mathcal{MNM} satisfies s -detailed balance thus fixes ρ_β . With contradiction assume that \mathcal{MNM} has two different fixed states ρ_1 and ρ_2 , thus

$$0 < \|\rho_1 - \rho_2\|_{*s} = \|\mathcal{MNM}(\rho_1 - \rho_2)\|_{*s}. \quad (102)$$

If $\mathcal{M}(\rho_1 - \rho_2) = 0$, then the above equation implies $0 < \|\rho_1 - \rho_2\|_{*s} = 0$ which leads to a contradiction. Otherwise assume $\mathcal{M}(\rho_1 - \rho_2) \neq 0$. Since \mathcal{M} is a quantum channel thus trace-preserving, we have $\mathcal{M}(\rho_1 - \rho_2)$ is traceless. Then use Lemma 17 for $\mathcal{M}, \mathcal{N}, \mathcal{M}$ sequentially we have that

$$\|\mathcal{M}\mathcal{N}\mathcal{M}(\rho_1 - \rho_2)\|_{*s} \leq \|\mathcal{N}\mathcal{M}(\rho_1 - \rho_2)\|_{*s} < \|\mathcal{M}(\rho_1 - \rho_2)\|_{*s} \leq \|\rho_1 - \rho_2\|_{*s}. \quad (103)$$

It suffices to notice that Eqs. (102)(103) lead to a contradiction $\|\rho_1 - \rho_2\|_{*s} < \|\rho_1 - \rho_2\|_{*s}$. Thus we conclude that $\mathcal{M}\mathcal{N}\mathcal{M}$ has a unique fixed state ρ_β .

Since $\mathcal{M}\mathcal{N}\mathcal{M}$ satisfies s -detailed balance and is a quantum channel, from Lemma 16 (4) we know that its spectrum lies in $[-1, 1]$. To show that its spectrum can be further restricted to be in $[0, 1]$ it suffices to prove all its eigenvalue are non-negative.

By Fact 1 we know that $\mathcal{M}\mathcal{N}\mathcal{M}$ has the same spectrum as $\mathcal{M}^\dagger \mathcal{N}^\dagger \mathcal{M}^\dagger$. Let X be an eigenvector of $\mathcal{M}^\dagger \mathcal{N}^\dagger \mathcal{M}^\dagger$ with eigenvalue λ . By assumption the spectrum of \mathcal{N} lies in $[0, 1]$, from Lemma 16 (3) we know the spectrum of \mathcal{N}^\dagger also lies in $[0, 1]$. Thus

$$\lambda = \frac{\langle X, \mathcal{M}^\dagger \mathcal{N}^\dagger \mathcal{M}^\dagger(X) \rangle_s}{\langle X, X \rangle_s} = \frac{\langle \mathcal{M}^\dagger(X), \mathcal{N}^\dagger \mathcal{M}^\dagger(X) \rangle_s}{\langle X, X \rangle_s} \geq 0, \quad (104)$$

■

Lemma 18 *Let \mathcal{N} be a quantum channel satisfying KMS detailed balance with respect to ρ_β , has ρ_β as its unique fixed state and has spectrum contained in $[0, 1]$. Then we have that*

$$\left(\frac{1}{\text{gap}(\mathcal{N})} - 1 \right) \log \left(\frac{1}{\epsilon} \right) \leq t_{mix}(\epsilon) \leq \frac{1}{\text{gap}(\mathcal{N})} \log \left(\frac{1}{\epsilon \sigma_{min}} \right). \quad (105)$$

Proof: To ease notation, in the following we denote $\Delta := \text{gap}(\mathcal{N})$.

(i) Proof for the lower bound. Denote the eigenvalues of \mathcal{N}^\dagger as $\gamma_1 = 1 > \gamma_2 \dots \geq 0$, and the corresponding eigenstate $Z_1 = I, Z_2, \dots$. Note that since \mathcal{N}^\dagger is Hermitian-preserving, the eigenstates $\{Z_j\}_j$ can be chosen to be Hermitian matrices. Indeed, suppose Z_j is not Hermitian. Denote the Kraus operator of the quantum channel \mathcal{N} is $\{K_u\}_u$, one can see that Z_j^\dagger is also an eigenstate of \mathcal{N}^\dagger with eigenvalue γ_j :

$$\gamma_j Z_j = \mathcal{N}^\dagger(Z_j) = \sum_u K_u^\dagger Z_j K_u \quad \Rightarrow \quad \gamma_j Z_j^\dagger = \sum_u K_u^\dagger Z_j^\dagger K_u = \mathcal{N}^\dagger(Z_j^\dagger). \quad (106)$$

where we use γ_j is real. Therefore the eigenstates Z_j, Z_j^\dagger can be replaced by the Hermitian matrices $Z_j + Z_j^\dagger, i(Z_j - Z_j^\dagger)$, which are also eigenstates of \mathcal{N}^\dagger with eigenvalue γ_j .

Let ρ be any initial state, consider the eigenstate Z_2 with eigenvalue γ_2 , for any t , we have that

$$\gamma_2^t \text{tr}(\rho Z_2) = \text{tr} \left(\rho (\mathcal{N}^\dagger)^t (Z_2) \right) = \text{tr} \left(\mathcal{N}^t(\rho) Z_2 \right) \quad (107)$$

$$= \text{tr} \left((\mathcal{N}^t(\rho) - \rho_\beta) Z_2 \right) \quad (108)$$

$$\leq \|\mathcal{N}^t(\rho) - \rho_\beta\|_1 \|Z_2\| \quad (109)$$

where Eq. (108) comes from the fact that Z_1 and Z_2 are orthogonal w.r.t. the weighted inner product,

$$\text{tr} \left(Z_1^\dagger \rho_\beta^{\frac{1}{2}} Z_2 \rho_\beta^{\frac{1}{2}} \right) = 0 \quad \Rightarrow \quad \text{tr}(\rho_\beta Z_2) = 0.$$

Since Z_2 is a Hermitian matrix, one can choose the quantum state ρ such that $\text{tr}(\rho Z_2) = \|Z_2\|$. Thus Eq. (109) implies that for such ρ ,

$$\gamma_2^t = (1 - \Delta)^t \leq \|\mathcal{N}^t(\rho) - \rho_\beta\|_1. \quad (110)$$

Thus

$$\log(\epsilon^{-1}) \leq t_{mix}(\epsilon) \log \left(\frac{1}{1 - \Delta} \right) \leq t_{mix}(\epsilon) \left(\frac{\Delta}{1 - \Delta} \right). \quad (111)$$

which completes the proof.

(ii) Proof for the upper bound. Using the χ_α^2 -contraction for $\alpha = \frac{1}{2}$ (See Theorem 9, [39]), we have that for any initial state ρ and any time t ,

$$\|\mathcal{N}^t(\rho) - \rho_\beta\|_1 \leq (1 - \Delta)^t \sqrt{\chi^2(\rho, \rho_\beta)} \leq e^{-\Delta t} \sqrt{\chi^2(\rho, \rho_\beta)}, \quad (112)$$

where

$$\sup_{\rho} \chi^2(\rho, \rho_\beta) = \sup_{\rho} \text{tr}(\rho \rho_\beta^{-\frac{1}{2}} \rho \rho_\beta^{-\frac{1}{2}}) - 1 = \sigma_{\min}^{-1} - 1. \quad (113)$$

Thus

$$t_{\text{mix}}(\epsilon) \leq \Delta^{-1} \log \left(\frac{1}{\epsilon \sqrt{\sigma_{\min}}} \right) \leq \Delta^{-1} \log \left(\frac{1}{\epsilon \sigma_{\min}} \right). \quad \blacksquare$$

C Examples for exponential decay of commutator norm

Recall that we use H and β to denote a local Hamiltonian and an inverse temperature, and write $\rho_\beta = \exp(-\beta H)/Z_\beta$ for the corresponding Gibbs state. In this section we give two examples where the commutator norm $\|\llbracket \hat{O}(\tau), \rho_\beta \rrbracket\|_1$ decays exponentially:

(i1) If H is the 2D Toric code and O is single-Pauli X , then $\forall \beta$, $\|\llbracket \hat{O}(\tau), \rho_\beta \rrbracket\|_1 \leq 2e^{-1/\tau^2}$.

(i2) Consider H is a Hamiltonian where there is a constant energy gap c between the ground energy and the first excited energy. Consider zero-temperature $\beta = +\infty$, where the Gibbs state ρ_β becomes the uniform mixture over the ground states. Then for any observable O with $\|O\| \leq 1$, we have $\|\llbracket \hat{O}(\tau), \rho_\beta \rrbracket\|_1 \leq 2e^{-c^2/(4\tau^2)}$.

To see that (i1) and (i2) hold, one can introduce a quantity that characterizes the extent to which O disturbs the eigenspaces. In particular, define

$$\mathcal{J}_O(\tau) := \sum_k p_k \exp\left(-\frac{\nu_k^2}{4\tau^2}\right), \quad (114)$$

where $p_k = \frac{\dim(\Pi_k) e^{-\beta E_k}}{Z_\beta}$ and the sum runs over all distinct eigenspaces of H , note that $\sum_k p_k = 1$. The quantity ν_k denotes the minimal nonzero energy change induced by O when starting from energy E_k . That is, $\nu_k := \min\left\{ |E_i - E_k| \mid E_i \in \text{Spec}(H), E_i \neq E_k, \Pi_i O \Pi_k \neq 0 \right\}$. One can check that

- If O induces constant energy changes for any eigenstate, i.e. $\nu_k = \mathcal{O}(1)$ for all k , e.g. consider H as the 2D Toric code and O as a single-qubit Pauli X , then we have $\nu_k = 2$ for all k , thus $\mathcal{J}_O(\tau) = \exp(-1/\tau^2)$.
- If there is a constant energy gap c between the ground energy and the first excited energy and the temperature is extremely low as $\beta = +\infty$, then for any O , $\mathcal{J}_O(\tau) = \exp(-c^2/(4\tau^2))$.

To see that (i1)(i2) hold, it suffices to note that the commutator norm is upper bounded by this quantity,

$$\|\llbracket \hat{O}(\tau), \rho_\beta \rrbracket\|_1 \leq 2 \mathcal{J}_O(\tau). \quad (115)$$

Proof: Recall that the definition of O_ν as in Eq. (77). First note that for any k , we have

$$O_0 \Pi_k = \Pi_k O \Pi_k = \Pi_k O_0,$$

thus

$$\llbracket \hat{O}(\tau), \rho_\beta \rrbracket = \llbracket \hat{O}(\tau) - O_0, \rho_\beta \rrbracket. \quad (116)$$

Let $|\psi_k\rangle$ be an eigenstate of H with energy E_k . By Eq. (77), one can check that

$$|\Phi_k(\tau)\rangle := \left(\hat{O}(\tau) - O_0 \right) |\psi_k\rangle = \sum_{j: j \neq k; \Pi_j O \Pi_k \neq 0} \exp\left(-\frac{(E_j - E_k)^2}{4\tau^2}\right) \Pi_j O |\psi_k\rangle. \quad (117)$$

Recall that $\|O\| \leq 1$. Thus we have

$$\| |\Phi_k(\tau)\rangle \|^2 = \langle \psi_k | O \left(\sum_{j: j \neq k; \Pi_j O \Pi_k \neq 0} \exp\left(-\frac{(E_j - E_k)^2}{2\tau^2}\right) \Pi_j \right) O |\psi_k\rangle \quad (118)$$

$$\leq \left\| \sum_{j: j \neq k, \langle \psi_j | O | \psi_k \rangle \neq 0} \exp\left(-\frac{(E_j - E_k)^2}{2\tau^2}\right) \Pi_j \right\| \quad (119)$$

$$= \exp\left(-\frac{\nu_k^2}{2\tau^2}\right). \quad (120)$$

Thus

$$\left\| \left[\hat{O}(\tau) - O_0, |\psi_k\rangle \langle \psi_k| \right] \right\|_1 \leq 2 \| |\Phi_k(\tau)\rangle \langle \psi_k| \|_1 \leq 2 \| |\Phi_k(\tau)\rangle \| \leq 2 \exp\left(-\frac{\nu_k^2}{4\tau^2}\right). \quad (121)$$

To prove the Lemma it suffices to express ρ_β in the eigenstate of H and use triangle inequality for the trace norm. \blacksquare

D Gaussian-filtered quantum phase estimation (GQPE)

In this section, we present a detailed discretization scheme for the idealized Gaussian-filtered quantum phase estimation described in Section 6.1. In particular, Sections D.1 and D.2 describe the discretization and its implementation on a qubit-based quantum computer, with the parameters summarized in Algorithm 2. From Section D.3 onward, we provide a rigorous resource analysis that establishes Theorem 3.

D.1 Implementation for Idealized Gaussian Filtered quantum phase estimation

To build intuition, here we provide an (imprecise) explanation of the implementation of the idealized Gaussian-filtered quantum phase estimation, assuming the ancilla system takes continuous values, i.e., the quantum channel \mathcal{M}_* introduced in Section 6.1. In the following section, we will discretize this process for implementation on qubits and carefully analyze the performance of the discretized version.

Define the Gaussian filter $g(\omega)$ and its Fourier transform:

$$g_\gamma(\omega) = \frac{1}{\sqrt{\gamma\sqrt{2\pi}}} e^{-\omega^2/4\gamma^2}, \quad \hat{g}_\gamma(\xi) = \int_{-\infty}^{\infty} e^{-2\pi i \xi \omega} g_\gamma(\omega) d\omega = \left(2\sqrt{2\pi}\gamma\right)^{1/2} e^{-4\pi^2\gamma^2\xi^2}. \quad (122)$$

The measurement \mathcal{M}_* can be implemented in the following way. Consider two registers and an input state $|\Psi\rangle$ on register 1,

1. Prepare a resource state $|\hat{G}_*\rangle$ on register 2 where $|\hat{G}_*\rangle := \int_{\xi=-\infty}^{+\infty} \hat{g}_\gamma(\xi) |\xi\rangle d\xi$.
2. Define controlled Hamiltonian evolution w.r.t. O as $W_* := \int_{\xi=-\infty}^{+\infty} e^{-2\pi i \xi O} \otimes |\xi\rangle\langle\xi|$. First perform controlled Hamiltonian evolution W_* on $|\Psi\rangle \otimes |\hat{G}_*\rangle$, then perform the inverse Fourier transform on register 2, which results in the state

$$|\tilde{\Psi}_*\rangle := \int_{\omega=-\infty}^{\infty} \left(\int_{\xi=-\infty}^{\infty} e^{2\pi i \xi \omega} \hat{g}_\gamma(\xi) e^{-2\pi i \xi O} d\xi \right) |\Psi\rangle \otimes |\omega\rangle, \quad (123)$$

$$= \frac{1}{\sqrt{\gamma\sqrt{2\pi}}} \int_{\omega=-\infty}^{\infty} \exp\left[-\frac{(\omega - O)^2}{4\gamma^2}\right] |\Psi\rangle \otimes |\omega\rangle; \quad (124)$$

3. Measuring the readout register (i.e., $|\omega\rangle$) in computational basis.

D.2 Circuit Implementation on qubits

In this section we implement a measurement \mathcal{M} on qubit systems which corresponds to a discretization of the idealized measurement \mathcal{M}_* .

Recall Eq. (123) that describes the ideal target state,

$$|\tilde{\Psi}_*\rangle := \int_{\omega=-\infty}^{\infty} \left(\int_{\xi=-\infty}^{\infty} e^{2\pi i \xi \omega} \hat{g}_\gamma(\xi) e^{-2\pi i \xi O} d\xi \right) |\Psi\rangle \otimes |\omega\rangle$$

To perform numerical integration, we discretize this double integral on the following quadrature points ($0 \leq j, \ell \leq N-1$):

$$\omega_j = \left(j - \frac{N}{2} \right) h, \quad \xi_\ell = \left(\ell - \frac{N}{2} \right) h,$$

where N is a discretization number and $h > 0$ is a step size. Their values will be specified later. The resulting numerical summation reads:

$$S_h^{[N]} = \sum_{j=0}^{N-1} \sqrt{h} \left(\sum_{\ell=0}^{N-1} h e^{2\pi i \xi_\ell \omega_j} \hat{g}_\gamma(\xi_\ell) e^{-2\pi i \xi_\ell O} \right) |\Psi\rangle \otimes |j\rangle, \quad (125)$$

Here we use $|j\rangle$ to denote $|\omega_j\rangle$. Note that the outer integral with respect to ω has a measure element \sqrt{h} to guarantee L^2 -normalization of quantum states, and the inner integral (for the inverse Fourier transform) has a measure element h .

For convenience, in what follows, we assume there is a positive integer m and $h = 2^{-m}$. We also choose the discretization number such that

$$N = \frac{1}{h^2} = 2^{2m}, \quad (126)$$

so that the energy readout register $\{j\}_{j=0}^{N-1}$ can be represented using $2m$ qubits. It is worth noting that $S_h^{[N]}$ is not a quantum state as it does not have a unit 2-norm:

$$C_h^{[N]} := \|S_h^{[N]}\| = \sqrt{h^3 N \sum_{\ell=1}^{N-1} |\hat{g}_\gamma(\xi_\ell)|^2} = \sqrt{h \sum_{\ell=1}^{N-1} |\hat{g}_\gamma(\xi_\ell)|^2}. \quad (127)$$

While the normalization factor $C_h^{[N]}$ is not unit, it converges exponentially fast to 1 as we increase N due to the rapid decay of $|\hat{g}_\gamma|^2(\xi)$, as we will show later in the proof analysis. Define the following two quantum operations:

- A (shifted) quantum Fourier transform:

$$\mathcal{F}_s |\ell\rangle \mapsto \frac{1}{\sqrt{N}} \sum_{j=0}^{N-1} \exp\left(\frac{2\pi i(\ell - N/2)(j - N/2)}{N}\right) |j\rangle. \quad (128)$$

Since we choose $N = 1/h^2$, this sQFT implements:

$$\mathcal{F}_s |\ell\rangle \mapsto h \sum_{j=0}^{N-1} e^{2\pi i \xi_\ell \omega_j} |j\rangle.$$

Note that $\frac{2\pi i(\ell - N/2)(j - N/2)}{N} = \frac{2\pi i \ell j}{N} - \pi i(\ell + j) + \frac{\pi i N}{2}$. Thus \mathcal{F}_s can be implemented by applying appropriate diagonal phase gates, then performing the standard quantum Fourier transform, up to a global phase $e^{\pi i N/2}$.

- A controlled unitary (i.e., select oracle):

$$W = \sum_{\ell=0}^{N-1} e^{-2\pi i \xi_\ell O} \otimes |\ell\rangle\langle\ell| = \sum_{\ell=0}^{N-1} e^{-2\pi i(\ell - N/2)hO} \otimes |\ell\rangle\langle\ell|. \quad (129)$$

We are now ready to implement the measurement \mathcal{M} on qubits as required for Theorem 3. The corresponding quantum circuit is summarized in Algorithm 2.

Algorithm 2 Implementation of Gaussian Filtered Quantum Phase estimation (GQPE) \mathcal{M}

Inputs: an observable O with $\|O\| \leq \kappa$, a quantum state $|\Psi\rangle$, a precision parameter ϵ , $2m$ ancilla qubits, and a parameter $\gamma > 0$ (specified in Eqs. (133)(136)).

Outputs: a measurement outcome $W \in \mathbb{R}$.

Registers: Register 1 is of n qubits initialized as $|\Psi\rangle$; Register 2 is of $2m$ ancillary qubits.

- 1: Normalize O by setting $\tilde{O} = O/\kappa$.
- 2: Denote $N = 2^{2m}$ and $h = 1/\sqrt{N} = 1/2^m$.
- 3: Prepare a Gaussian resource state $|\hat{G}\rangle$ on register 2, defined as (where ξ_ℓ and $C_h^{[N]}$ are the same as in Eq. (127))

$$|\hat{G}\rangle = \frac{1}{C_h^{[N]}} \sum_{\ell=1}^{N-1} \sqrt{h} \hat{g}_\gamma(\xi_\ell) |\ell\rangle. \quad (130)$$

- 4: Apply the controlled unitary W and $I \otimes \mathcal{F}_s$ to $|\Psi\rangle \otimes |\hat{G}\rangle$ and get the target state $|\hat{\Psi}\rangle$, where \mathcal{F}_s defined in Eq.(128) and W defined in Eq. (129) w.r.t. \tilde{O} :

$$\begin{aligned} |\Psi\rangle \otimes |\hat{G}\rangle &\xrightarrow{W} \frac{\sqrt{h}}{C_h^{[N]}} \sum_{\ell=1}^{N-1} \hat{g}_\gamma(\xi_\ell) e^{-2\pi i \xi_\ell \tilde{O}} |\Psi\rangle \otimes |\ell\rangle \\ &\xrightarrow{I \otimes \mathcal{F}_s} \frac{h^{3/2}}{C_h^{[N]}} \sum_{\ell=1}^{N-1} \sum_{j=0}^{N-1} e^{2\pi i \xi_\ell \omega_j} \hat{g}_\gamma(\xi_\ell) e^{-2\pi i \xi_\ell \tilde{O}} |\Psi\rangle \otimes |j\rangle = |\hat{\Psi}\rangle. \end{aligned} \quad (131)$$

- 5: Measure register 2 in the computational basis and obtain an outcome $j \in \{0, \dots, N-1\}$. (Conditioned on this outcome, the post-measurement state on register 1 is proportional to $O_j |\Psi\rangle$, for O_j defined in Eq.(137).) Let $\omega = (j - \frac{N}{2}) h$, and we define

$$Z := \begin{cases} \omega & -2 \leq \omega \leq 2, \\ 0 & \text{otherwise.} \end{cases} \quad (132)$$

- 6: Output the measurement outcome: $W = \kappa Z$.

D.3 Resource Estimation: Proof of Theorem 3

D.3.1 Outline of proof

Theorem 3 guarantees that the measurement \mathcal{M} recovers the observable value of O . Furthermore, the measurement procedure leaves the Gibbs state ρ_β undisturbed if $[\rho_\beta, O] = 0$; and only slightly perturbs ρ_β when $[\rho_\beta, O]$ is small. We demonstrate those by characterizing the expectation, variance, covariance, and commutativity properties of the measurement channel \mathcal{M} . Specifically, the following subsections establish a series of technical results regarding the measurement statistics:

- Expectation and variance of Z : Corollary 20,
- Covariance of two consecutive Z 's: Proposition 23,
- Commutative properties of \mathcal{M} : Proposition 25.

Note that the above technical lemmas all assume that the spectral norm of the observable operator O is bounded by 1. In what follows, we show that the error bound for case $\|O\| \leq 1$ implies the desired bound for the general case $\|O\| \leq \kappa = \text{poly}(n)$. More specifically, for a given precision parameter ϵ , we consider the normalized observable \tilde{O} and a new precision parameter $\tilde{\epsilon}$, where

$$\tilde{O} = O/\kappa, \quad \tilde{\epsilon} = \epsilon/\kappa.$$

Let Z be the raw readout in Algorithm 2, as given in Eq. (132). By Corollary 20, we can choose

$$\gamma^{-1} = \mathcal{O}(\kappa \log^{1/2}(1/\tilde{\epsilon})), \quad h^{-1} = \mathcal{O}(\gamma^{-1} \log^{1/2}(\gamma^2/\tilde{\epsilon})) \quad (133)$$

such that

$$|\mathbb{E}[Z] - \mathbb{E}_\rho[\tilde{O}]| \leq \tilde{\epsilon}, \quad |\text{Var}[Z] - \text{Var}_\rho[\tilde{O}]| \leq 3/\kappa^2, \quad (134)$$

which immediately implies that the final output $W = \kappa Z$ satisfies:

$$|\mathbb{E}[W] - \mathbb{E}_\rho[O]| \leq \epsilon, \quad |\text{Var}[W] - \text{Var}_\rho[O]| \leq 3. \quad (135)$$

The covariance property and the commutative property directly follow from this error analysis, as discussed in Proposition 23 and Proposition 25.

Implementation cost. With the parameter choice as in Eq. (133), we have the number of ancilla qubits $2m$ and the maximal Hamiltonian simulation time t_{\max} (of the original observable O) as follows:

$$m = \log_2(1/h) = \mathcal{O}(\log(\kappa) + \log \log(\epsilon^{-1})), \quad t_{\max} = \frac{Nh}{2\kappa} = \mathcal{O}(\log(\kappa) + \log(\epsilon^{-1})) \quad (136)$$

The Gaussian resource state $|\tilde{G}\rangle$ can be prepared using the methods in [40, 37], with gate complexity $\text{poly}(m) = \text{poly} \log(\kappa) + \text{poly} \log(\epsilon^{-1})$.

D.3.2 Expectation and variance

In the following analysis, we define a new operator for each $j \in \{0, \dots, N-1\}$:

$$O_j := O_{w_j} := \frac{h^{3/2}}{C_h^{[N]}} \sum_{\ell=1}^{N-1} e^{2\pi i \xi_\ell (\omega_j - \tilde{O})} \hat{g}_\gamma(\xi_\ell) = \frac{h^{3/2}}{C_h^{[N]}} \sum_{k=1-N/2}^{N/2-1} e^{2\pi i kh (\omega_j - \tilde{O})} \hat{g}_\gamma(kh) \quad (137)$$

One can check that Algorithm 2 implement a quantum channel \mathcal{M} where

$$\mathcal{M}[\rho] = \sum_{j=0}^{N-1} O_{w_j} \rho O_{w_j}^\dagger. \quad (138)$$

Proposition 19 *Let O be an observable with $\|O\| \leq 1$. There exist parameter choices*

$$\gamma^{-1} = \mathcal{O}(\log^{1/2}(1/\epsilon)), \quad h^{-1} = \mathcal{O}(\gamma^{-1} \log^{1/2}(\gamma^2/\epsilon)) \quad (139)$$

such that

$$\left\| \sum_{|\omega_j| \leq 2} \omega_j O_j^\dagger O_j - O \right\| \leq \epsilon, \quad \left\| \sum_{|\omega_j| \leq 2} \omega_j^2 O_j^\dagger O_j - (O^2 + \gamma^2 I) \right\| \leq 2\gamma^2. \quad (140)$$

The proof of Proposition 19 is postponed to the end of this subsection. Below, we state an immediate corollary that characterizes the measurement statistics Z .

Corollary 20 (Expectation and Variance) *Let O be an observable with $\|O\| \leq 1$. Define*

$$\mathbb{E}_\rho[O] := \text{tr}[\rho O], \quad \text{Var}_\rho[O] := \mathbb{E}_\rho[O^2] - \mathbb{E}_\rho[O]^2$$

For any quantum state ρ , there exists parameter choices of γ and h as in Eq. (139) such that the measurement statistics Z in Algorithm 2 satisfy

$$|\mathbb{E}[Z] - \text{tr}[\rho O]| \leq \epsilon, \quad |\text{Var}[Z] - \text{Var}_\rho[O]| \leq 3\gamma^2. \quad (141)$$

Proof: Given a quantum state ρ , the expectation and variance of the random variable Z are:

$$\begin{aligned} \mathbb{E}[Z] &= \sum_{-2 \leq \omega_j \leq 2} \omega_j \text{tr}[O_j^\dagger O_j \rho] = \text{tr} \left[\left(\sum_{|\omega_j| \leq 2} \omega_j O_j^\dagger O_j \right) \rho \right], \\ \text{Var}[Z] &= \mathbb{E}[Z^2] - \mathbb{E}[Z]^2, \quad \mathbb{E}[Z^2] = \text{tr} \left[\left(\sum_{|\omega_j| \leq 2} \omega_j^2 O_j^\dagger O_j \right) \rho \right]. \end{aligned}$$

Then, the proof follows from Proposition 19 and the triangle inequality. Under the assumption that $\epsilon \ll \gamma^2$, the error in the squared expectation value can be bounded by an additional term of γ^2 . \blacksquare

Lemma 21 Let O be an observable with $\|O\| \leq 1$. For any $\gamma > 0$, and $-2 \leq \omega \leq 2$, define

$$O_\omega := \frac{h^{3/2}}{C_h^{[N]}} \sum_{\ell=1}^{N-1} e^{2\pi i \xi_\ell (\omega - O)} \widehat{g}_\gamma(\xi_\ell), \quad (142)$$

where h , $C_h^{[N]}$, and ξ_ℓ are the same as in Eq. (137). Clearly, we have $O_{\omega_j} = O_j$ for $|\omega_j| \leq 2$. Then, there is an absolute constant $c > 0$ such that for any $\gamma \leq \frac{1}{2\sqrt{2}\pi}$, we can choose $h \leq c/\gamma$ and

$$\left\| O_\omega - \sqrt{h} g_\gamma(\omega - O) \right\| \leq \frac{12h^{1/2}}{\gamma^{1/2}} e^{-\frac{1}{16\gamma^2 h^2}} + \frac{h^{3/2}}{2\gamma^{3/2}} e^{-\frac{2\pi^2 \gamma^2}{h^2}}. \quad (143)$$

Proof: To ease notation, in the proof we abbreviate $g_\gamma, \widehat{g}_\gamma$ as g and \widehat{g} . Since O is a Hermitian operator, it suffices to prove Eq. (143) in the eigenbasis of O . In the following argument, we demonstrate that the lemma is true in any one-dimensional eigensubspace of O . We first define

$$I_h^{[N]} := h \sum_{k=-N/2+1}^{N/2-1} e^{2\pi i kh(\omega - E)} \widehat{g}(kh),$$

and by the triangle inequality, we have

$$\left| \frac{h^{3/2}}{C_h^{[N]}} \sum_{\ell=1}^{N-1} e^{2\pi i \xi_\ell (\omega - E)} \widehat{g}(\xi_\ell) - \sqrt{h} g(\omega - E) \right| \leq \sqrt{h} \left[\left| \frac{1}{C_h^{[N]}} \left| I_h^{[N]} - g(\omega - E) \right| \right| + \left| \frac{1}{C_h^{[N]}} - 1 \right| |g(\omega - E)| \right]. \quad (144)$$

1. First, we estimate the quadrature error $|I_h^{[N]} - g(\omega - E)|$. For simplicity, we denote

$$\varphi(x) = e^{2\pi i x(\omega - E)} \widehat{g}(x).$$

Note that $\varphi(\xi)$ is an analytic function on \mathbb{R} and its Fourier transform is

$$\widehat{\varphi}(y) = \int_{-\infty}^{\infty} e^{-2\pi i xy} \varphi(x) dx = g(\omega - E - y), \quad (145)$$

$$\text{in particular } \widehat{\varphi}(0) = \int_{-\infty}^{\infty} \varphi(x) dx = g(\omega - E). \quad (146)$$

Then, the numerical sum can be simply written as $I_h^{[N]} = h \sum_{k=-N/2}^{N/2-1} \varphi(kh)$. By Lemma 28,

$$|I_h^{[N]} - g(\omega - E)| \leq \sum_{n=-\infty, n \neq 0}^{\infty} \|\widehat{\varphi}(n/h)\| + h \sum_{|k| \geq N/2} \|\varphi(kh)\| \quad (147)$$

Since $|\omega - E| \leq 3$, by choosing $h \leq 1/6$,

$$\left\| \widehat{\varphi}\left(\frac{n}{h}\right) \right\| = \left\| g\left(\omega - E - \frac{n}{h}\right) \right\| \leq \left\| g\left(\frac{|n| - 1/2}{h}\right) \right\| \leq \frac{1}{\sqrt{\gamma}\sqrt{2\pi}} \exp\left(-\frac{(|n| - 1/2)^2}{4h^2\gamma^2}\right).$$

Plugging this upper bound into Eq. (147) and invoking Lemma 29, we have

$$\begin{aligned} |I_h^{[N]} - g(\omega - E)| &\leq \frac{2}{\sqrt{\gamma}\sqrt{2\pi}} \sum_{n=1}^{\infty} \exp\left(-\frac{(|n| - 1/2)^2}{4h^2\gamma^2}\right) + 2h \left(2\sqrt{2\pi}\gamma\right)^{1/2} \sum_{k \geq N/2} e^{-4\pi^2\gamma^2 h^2 k^2} \\ &\leq \frac{6}{\sqrt{\gamma}\sqrt{2\pi}} e^{-\frac{1}{16\gamma^2 h^2}} + 2h \left(2\sqrt{2\pi}\gamma\right)^{1/2} \left(1 + \frac{1}{4\pi^2\gamma^2}\right) e^{-\frac{\pi^2\gamma^2}{h^2}} \\ &\leq \frac{6}{\sqrt{\gamma}\sqrt{2\pi}} e^{-\frac{1}{16\gamma^2 h^2}} + \frac{h\sqrt{2\sqrt{2\pi}}}{\pi^2\gamma^{3/2}} e^{-\frac{\pi^2\gamma^2}{h^2}}. \end{aligned}$$

Note that we use $4\pi^2\gamma^2 \leq 1$ in the last step, and the first part in the second inequality follows from

$$\sum_{n=1}^{\infty} \exp\left(-\frac{(|n| - 1/2)^2}{4h^2\gamma^2}\right) \leq e^{-\frac{1}{16h^2\gamma^2}} + \sum_{n=1}^{\infty} e^{-\frac{n^2}{4h^2\gamma^2}} \leq e^{-\frac{1}{16h^2\gamma^2}} + (1 + 2h^2\gamma^2) e^{-\frac{1}{4h^2\gamma^2}} \leq 3e^{-\frac{1}{16h^2\gamma^2}}.$$

In the third step, we use Lemma 29; the last step follows from the fact that $2h^2\gamma^2 \leq 1$.

2. Next, we consider the normalization error $|1/C_h^{[N]} - 1|$. We denote a new integrand function $\phi(x) = |\widehat{g}(x)|^2 = 2\sqrt{2\pi}\gamma e^{-8\pi^2\gamma^2x^2}$. This is a Gaussian density function, and its Fourier transform is $\widehat{\phi}(y) = e^{-y^2/(8\gamma^2)}$. Again, by Lemma 28, we have

$$\begin{aligned} \left| \left(C_h^{[N]} \right)^2 - 1 \right| &\leq \sum_{n=-\infty, n \neq 0}^{\infty} e^{-n^2/(8h^2\gamma^2)} + 2h \sum_{k \geq N/2} 2\sqrt{2\pi}\gamma e^{-8\pi^2\gamma^2k^2h^2} \\ &\leq 2 \sum_{n \geq 1} e^{-n/(8h^2\gamma^2)} + 4\sqrt{2\pi}h\gamma \sum_{k \geq N/2} e^{-8\pi^2\gamma^2h^2k^2} \\ &\leq \frac{2}{e^{\frac{1}{8h^2\gamma^2}} - 1} + 4\sqrt{2\pi}h\gamma \left(1 + \frac{1}{8\pi^2\gamma^2} \right) e^{-2\pi^2\gamma^2/h^2} \leq 3e^{-\frac{1}{8\gamma^2h^2}} + \frac{h\sqrt{2}}{\pi^{3/2}\gamma} e^{-\frac{2\pi^2\gamma^2}{h^2}}. \end{aligned}$$

Note that $Nh^2 = 1$. We use Lemma 29 in the second inequality, and we assume $\gamma \leq \frac{1}{2\sqrt{2\pi}}$ in the last step.

3. Note that $g(\omega - E) \leq \frac{1}{\sqrt{\gamma\sqrt{2\pi}}}$. By the previous part, we can always choose $h \leq c/\gamma$ for an absolute constant $c > 0$ such that $|C_h^{[N]} - 1| \leq 1/2$. Then, we have

$$\begin{aligned} &\left| \frac{h^{3/2}}{C_h^{[N]}} \sum_{\ell=0}^{N-1} e^{2\pi i \xi_{\ell}(\omega - E)} \widehat{g}(\xi_{\ell}) - \sqrt{h}g(\omega - E) \right| \leq \\ &\sqrt{h} \left[2 \left(\frac{6}{\sqrt{\gamma\sqrt{2\pi}}} e^{-\frac{1}{16\gamma^2h^2}} + \frac{h\sqrt{2\sqrt{2\pi}}}{\pi^2\gamma^{3/2}} e^{-\frac{\pi^2\gamma^2}{h^2}} \right) + \frac{2}{\sqrt{\gamma\sqrt{2\pi}}} \left(3e^{-\frac{1}{8\gamma^2h^2}} + \frac{h\sqrt{2}}{\pi^{3/2}\gamma} e^{-\frac{2\pi^2\gamma^2}{h^2}} \right) \right] \\ &\leq \frac{12h^{1/2}}{\gamma^{1/2}} e^{-\frac{1}{16\gamma^2h^2}} + \frac{h^{3/2}}{2\gamma^{3/2}} e^{-\frac{2\pi^2\gamma^2}{h^2}}. \end{aligned}$$

This proves the lemma for any $-2 \leq \omega \leq 2$. ■

Lemma 22 *Let O be a quantum observable such that $\|O\| \leq 1$. Then, given an $\epsilon > 0$, there exists parameter choices of γ and h as in Eq. (139) such that*

$$\left\| h \sum_{|\omega_j| \leq 2} \omega_j g_{\gamma}^2(\omega_j - O) - O \right\| \leq \epsilon, \quad \left\| h \sum_{|\omega_j| \leq 2} \omega_j^2 g_{\gamma}^2(\omega_j - O) - (O^2 + \gamma^2 I) \right\| \leq \gamma^2. \quad (148)$$

Proof: To ease notation, in the proof, we abbreviate $g_{\gamma}, \widehat{g}_{\gamma}$ as g and \widehat{g} . Since O is Hermitian, it suffices to prove the lemma in the eigenbasis of O . By $\|O\| \leq 1$, it reduces to proving the following inequalities for any $-1 \leq E \leq 1$:

$$\left| h \sum_{|\omega_j| \leq 2} \omega_j g^2(\omega_j - E) - E \right| \leq \epsilon, \quad \left| h \sum_{|\omega_j| \leq 2} \omega_j^2 g^2(\omega_j - E) - (E^2 + \gamma^2) \right| \leq \gamma^2. \quad (149)$$

1. To prove the first part, we define the integrand function $\varphi(x) := xg^2(x-E) = \frac{x}{\gamma\sqrt{2\pi}} e^{-(x-E)^2/2\gamma^2}$, and its Fourier transform reads $\widehat{\varphi}(y) = (E - 2\pi i \gamma^2 y) e^{-2\pi i E y} e^{-2\pi^2 \gamma^2 y^2}$. We define:

$$I_h = h \sum_{k=-\infty}^{\infty} \varphi(kh), \quad (150)$$

By the triangle inequality:

$$\left| h \sum_{|\omega_j| \leq 2} \omega_j g^2(\omega_j - E) - E \right| \leq \left| h \sum_{|\omega_j| \leq 2} \omega_j g^2(\omega_j - E) - I_h \right| + |I_h - E|.$$

The first term can be bounded using the fact that $|E| \leq 1$,

$$\left| h \sum_{|\omega_j| \leq 2} \omega_j g^2(\omega_j - E) - I_h \right| \leq h \sum_{|jh| > 2} |\varphi(jh)| \quad (151)$$

$$\leq \frac{2h}{\gamma\sqrt{2\pi}} \sum_{j \geq 1} (2 + jh) e^{-(1+jh)^2/2\gamma^2} \leq \frac{2}{\sqrt{2\pi}} \left(\gamma + \sqrt{\frac{\pi}{2}} \right) e^{-\frac{1}{2\gamma^2}}. \quad (152)$$

The second term can be bounded using the Poisson summation formula,

$$|I_h - E| = \left| \sum_{n=-\infty, n \neq 0}^{\infty} \hat{\varphi}(n/h) \right| \leq \frac{8\pi\gamma^2}{h} \sum_{n=1}^{\infty} n e^{-2\pi^2\gamma^2 n^2/h^2} \quad (153)$$

$$\leq \frac{8\pi\gamma^2}{h} \frac{e^{-2\pi^2\gamma^2/h^2}}{(1 - e^{-2\pi^2\gamma^2/h^2})^2} \leq \frac{8\pi\gamma^2}{h(e^{2\pi^2\gamma^2/h^2} - 2)}, \quad (154)$$

where the second step assumes that $h \leq 2\pi\gamma^2$ (i.e., $2\pi\gamma^2/h \geq 1 \geq |E|$). Note that $h \geq e^{-\pi^2\gamma^2/h^2}$ for any $h \leq \min(1, \sqrt{2}\pi\gamma)$. We further require $h \leq \sqrt{2\pi\gamma}/\sqrt{\ln(4)}$ (i.e., $e^{2\pi^2\gamma^2/h^2} - 2 \leq \frac{e^{2\pi^2\gamma^2/h^2}}{2}$), and it follows that:

$$\frac{8\pi\gamma^2}{h(e^{2\pi^2\gamma^2/h^2} - 2)} \leq \frac{16\pi\gamma^2}{h e^{2\pi^2\gamma^2/h^2}} \leq \frac{16\pi\gamma^2}{e^{\pi^2\gamma^2/h^2}},$$

which is bounded by $\epsilon/2$ if we choose $1/h \geq \frac{1}{\pi\gamma} \log^{1/2}(32\pi\gamma^2/\epsilon)$. Combining the above error bounds, it turns out that if we choose

$$\frac{1}{\gamma} = \sqrt{2} \cdot \max \left(\pi, \log^{1/2} \left(\frac{4}{\epsilon} \right) \right), \quad \frac{1}{h} = \max \left(\pi, \frac{1}{\pi\gamma} \log^{1/2} \left(\frac{32\pi\gamma^2}{\epsilon} \right) \right),$$

we have $\left| h \sum_{|\omega_j| \leq 2} \omega_j g^2(\omega_j - E) - E \right| \leq \frac{\epsilon}{2} + \frac{\epsilon}{2} = \epsilon$.

2. To prove the second part, we first define the integrand function $\phi(x) := x^2 g^2(x - E) = \frac{x^2}{\gamma\sqrt{2\pi}} e^{-(x-E)^2/2\gamma^2}$. The Fourier transform of $\phi(x)$ is

$$\hat{\phi}(y) = (\gamma^2 + E^2 - 4\pi i E \gamma^2 y - 4\pi^2 \gamma^4 y^2) e^{-2\pi i E y} e^{-2\pi^2 \gamma^2 y^2}.$$

Note that $\int_{-\infty}^{\infty} \phi(x) dx = \hat{\phi}(0) = E^2 + \gamma^2$. We define $J_h = h \sum_{k=-\infty}^{\infty} \phi(kh)$, by the triangle inequality,

$$\left| h \sum_{|\omega_j| \leq 2} \omega_j^2 g^2(\omega_j - E) - (E^2 + \gamma^2) \right| \leq \left| h \sum_{|\omega_j| \leq 2} \omega_j^2 g^2(\omega_j - E) - J_h \right| + |J_h - (E^2 + \gamma^2)|.$$

The first term can be bounded using $|E| \leq 1$,

$$\left| h \sum_{|\omega_j| \leq 2} \omega_j^2 g^2(\omega_j - E) - J_h \right| \leq h \sum_{|jh| > 2} |\phi(jh)| \quad (155)$$

$$\leq \frac{2h}{\gamma\sqrt{2\pi}} \sum_{j \geq 1} (2 + jh)^2 e^{-(1+jh)^2/2\gamma^2} \leq \frac{64\gamma^3}{e\sqrt{2\pi}(1+h)} e^{-\frac{(h+1)^2}{4\gamma^2}}. \quad (156)$$

Again, we invoke the Poisson summation formula to bound the second term:

$$|J_h - (E^2 + \gamma^2)| = \sum_{n=-\infty, n \neq 0}^{\infty} \hat{\phi}(n/h) \leq \frac{4\pi^2\gamma^2}{h^2} \sum_{n=1}^{\infty} n^2 e^{-2\pi^2\gamma^2 n^2/h^2} \leq \frac{6\sqrt{2}h}{\pi\gamma}. \quad (157)$$

where the second step assumes that $h \leq \sqrt{2}\pi\gamma$ and the second to last step uses the inequality $\sum_{n \geq 1} n^2 e^{-a^2 n^2} \leq 6a^{-3}$ (for $a \geq 1$). By choosing

$$\gamma^{-1} = \mathcal{O} \left(\log^{1/2} (4\epsilon^{-1}) \right), \quad h^{-1} = \mathcal{O} \left(\gamma^{-1} \log^{1/2} (\gamma^2 \epsilon^{-1}) \right),$$

we have

$$\left| h \sum_{|\omega_j| \leq 2} \omega_j^2 g^2(\omega_j - E) - (E^2 + \gamma^2) \right| \leq \frac{64\gamma^3}{e\sqrt{2\pi}(1+h)} e^{-\frac{(h+1)^2}{4\gamma^2}} + \frac{6\sqrt{2}h}{\pi\gamma} \leq \frac{\gamma^2}{2} + \frac{\gamma^2}{2} \leq \gamma^2.$$

■

Now, we are ready to prove Proposition 19.

Proof: [of Proposition 19] To ease notation, in the proof we abbreviate $g_{\gamma}, \hat{g}_{\gamma}$ as g and \hat{g} .

1. By the triangle inequality, we have

$$\left\| \sum_{|\omega_j| \leq 2} \omega_j O_j^\dagger O_j - O \right\| \leq I_1 + I_2 + I_3, \quad (158)$$

where

$$\begin{aligned} I_1 &= \sum_{|\omega_j| \leq 2} |\omega_j| \|O_j - \sqrt{h}g(\omega_j - O)\|^2 \leq \frac{1152}{\gamma} e^{-\frac{1}{8\gamma^2 h^2}} + \frac{2h^2}{\gamma^3} e^{-\frac{4\pi^2 \gamma^2}{h^2}}, \\ I_2 &= 2\sqrt{h} \sum_{|\omega_j| \leq 2} |\omega_j| \|O_j - \sqrt{h}g(\omega_j - O)\| \|g(\omega_j - O)\| \leq \frac{1}{(2\pi)^{1/4}} \left(\frac{96}{\gamma} e^{-\frac{1}{16\gamma^2 h^2}} + \frac{4h}{\gamma^2} e^{-\frac{2\pi^2 \gamma^2}{h^2}} \right), \\ I_3 &= \left\| h \sum_{|\omega_j| \leq 2} \omega_j g^2(\omega_j - O) - O \right\|. \end{aligned}$$

We require $\gamma \leq \frac{1}{2\sqrt{2}\pi} < 1$, so

$$I_1 + I_2 \leq \frac{1213}{\gamma} e^{-\frac{1}{16\gamma^2 h^2}} + \frac{5h}{\gamma^3} e^{-\frac{4\pi^2 \gamma^2}{h^2}}.$$

Without loss of generality, we assume $h \leq 1$. So it suffices to choose

$$\gamma^{-1} = \mathcal{O}(\log^{1/2} \epsilon^{-1}), \quad (159)$$

$$h^{-1} = \max \left(4\gamma \log^{1/2} \left(\frac{4852}{\gamma \epsilon} \right), \frac{1}{2\pi\gamma} \log^{1/2} \left(\frac{20}{\gamma^2 \epsilon} \right) \right) = \mathcal{O}(\gamma^{-1} \log^{1/2}(\gamma^{-1}, \epsilon^{-1})), \quad (160)$$

to ensure that $I_1 + I_2 \leq \epsilon/2$. By Lemma 22, we can make $I_3 \leq \epsilon/2$ in the same parameter regime. This proves the first part of the theorem.

2. Similar to part 1, by the triangle inequality, we have

$$\left\| \sum_{|\omega_j| \leq 2} \omega_j^2 O_j^\dagger O_j - (O^2 + \gamma^2 I) \right\| \leq J_1 + J_2 + J_3, \quad (161)$$

where

$$\begin{aligned} J_1 &= \sum_{|\omega_j| \leq 2} \omega_j^2 \|O_j - \sqrt{h}g(\omega_j - O)\|^2 \leq \frac{2304}{\gamma} e^{-\frac{1}{8\gamma^2 h^2}} + \frac{4h^2}{\gamma^3} e^{-\frac{4\pi^2 \gamma^2}{h^2}}, \\ J_2 &= 2\sqrt{h} \sum_{|\omega_j| \leq 2} \omega_j^2 \|O_j - \sqrt{h}g(\omega_j - O)\| \|g(\omega_j - O)\| \leq \frac{1}{(2\pi)^{1/4}} \left(\frac{192}{\gamma} e^{-\frac{1}{16\gamma^2 h^2}} + \frac{8h}{\gamma^2} e^{-\frac{2\pi^2 \gamma^2}{h^2}} \right), \\ J_3 &= \left\| h \sum_{|\omega_j| \leq 2} \omega_j^2 g^2(\omega_j - O) - (O^2 + \gamma^2 I) \right\|. \end{aligned}$$

Similarly, we can make $J_1 + J_2 \leq \gamma^2$ by the specified parameters. choosing $h^{-1} = \gamma^{-1} \cdot \text{poly log}(\gamma^{-1})$. By Lemma 22, we can make $J_3 \leq \gamma^2$ by the choice of parameters. Combining these two parts together, we prove that

$$\left\| \sum_{|\omega_j| \leq 2} \omega_j^2 O_j^\dagger O_j - (O^2 + \gamma^2 I) \right\| \leq 2\gamma^2,$$

which immediately implies Eq. (140). This concludes the proof of part 2 of the theorem. ■

D.3.3 Covariance

Proposition 23 (Covariance) *Let O be an observable with $\|O\| \leq 1$. For any quantum state ρ , let Z be the measurement outcome from \mathcal{M} on ρ . Then, measuring the output state again using another \mathcal{M} , we obtain an outcome Z' . We have that,*

$$|\text{Cov}(Z, Z')| \leq \text{Var}[Z]. \quad (162)$$

Proof: [of Proposition 23] By definition,

$$\mathbb{E}[ZZ'] = \sum_{j,k} \tilde{\omega}_j \tilde{\omega}_k \mathbb{P}[Z = \omega_j, Z' = \omega_k],$$

where $\tilde{\omega}_j = \omega_j$ if $|\omega_j| \leq 2$; otherwise $\tilde{\omega}_j = 0$. By Lemma 24, all O_j commute with each other and $O_j = O_j^\dagger$. Suppose $|\psi\rangle$ is a common eigenvector of O_j^2 , w.r.t. eigenvalue p_j . Note that $\sum_j p_j = 1$ since $\sum_j O_j^2 = I$. Using Cauchy inequality we have that

$$\left(\sum_j (\tilde{\omega}_j - \mathbb{E}[Z]) p_j \right)^2 \leq \sum_j (\tilde{\omega}_j - \mathbb{E}[Z])^2 p_j \quad \Rightarrow \quad \left(\sum_j (\tilde{\omega}_j - \mathbb{E}[Z]) O_j^2 \right)^2 \leq \sum_j (\tilde{\omega}_j - \mathbb{E}[Z])^2 O_j^2. \quad (163)$$

Since all O_j commute with each other and $O_j = O_j^\dagger$, using $\text{tr}(A\rho B) = \text{tr}(BA\rho)$, one can check that

$$\text{Cov}(ZZ') = \text{tr} \left[\left(\sum_j (\tilde{\omega}_j - \mathbb{E}[Z]) O_j^2 \right) \left(\sum_k (\tilde{\omega}_k - \mathbb{E}[Z]) O_k^2 \right) \rho \right] \quad (164)$$

$$= \text{tr} \left[\left(\sum_j (\tilde{\omega}_j - \mathbb{E}[Z]) O_j^2 \right)^2 \rho \right] \quad (165)$$

$$\leq \text{tr} \left[\left(\sum_j (\tilde{\omega}_j - \mathbb{E}[Z])^2 O_j^2 \right) \rho \right] \quad (166)$$

$$= \text{Var}[Z]. \quad (167)$$

where in the inequality we use Eq. (163). Finally, notice that from Eq. (165) we have that $\text{Cov}(ZZ') \geq 0$. Thus from above equations we have proved $|\text{Cov}(ZZ')| \leq \text{Var}[Z]$. \blacksquare

Lemma 24 $\{O_j\}_j$ defined as in Eq. (138) commute with each other since each O_j is a function of the same Hermitian operator O . Besides, O_j is Hermitian.

Proof: O_j is Hermitian since \hat{g} is real and symmetric. More specifically,

$$O_j^\dagger = \frac{h^{3/2}}{C_h^{[N]}} \sum_{k=1-N/2}^{N/2-1} e^{-2\pi i kh(\omega_j - \tilde{O})} \hat{g}(kh) = \frac{h^{3/2}}{C_h^{[N]}} \sum_{k=1-N/2}^{N/2-1} e^{2\pi i kh(\omega_j - \tilde{O})} \hat{g}(-kh) = O_j,$$

Here, the second equality follows by relabeling $-k$ as k , and the last equality uses the symmetry $\hat{g}(x) = \hat{g}(-x)$. \blacksquare

D.3.4 Commutativity

In this section, we prove the commutativity property of GQPE in Theorem 3, where we assume $\|O\| \leq \kappa = 1$. To ease notation, define

$$\delta(\gamma, h) = \frac{12h^{1/2}}{\gamma^{1/2}} e^{-\frac{1}{16\gamma^2 h^2}} + \frac{h^{3/2}}{2\gamma^{3/2}} e^{-\frac{2\pi^2 \gamma^2}{h^2}}. \quad (168)$$

Recall that the parameters γ and h are chosen such that terms below scale as ϵ ,

$$\left\{ e^{-\mathcal{O}(\frac{1}{\gamma^2})}, e^{-\mathcal{O}(\frac{1}{\gamma^2 h^2})} \text{ and } e^{-\mathcal{O}(\frac{\gamma^2}{h^2})} \right\} \times \text{poly}(\gamma, h, h^{-1}, \gamma^{-1}).$$

Proposition 25 (Commutativity property) Suppose $\|O\| \leq 1$. For the parameter choices of γ and h given in Eq. (139), the quantum channel \mathcal{M} implemented by Algorithm 2 approximately fixes ρ when O and ρ approximately commute, in the sense that

$$\|\mathcal{M}[\rho] - \rho\|_1 \leq \epsilon^{-1} \text{poly log}(\epsilon^{-1}) \| [O, \rho] \|_1 + 5\epsilon. \quad (169)$$

First, we bound the leakage probability,

Lemma 26 (Leakage probability) Let O be an observable with $\|O\| \leq 1$. Given any quantum state ρ and an $\epsilon > 0$, for the parameter choices of γ and h given in Eq. (139), the probability of observing a value outside $[-2, 2]$ in the readout registers is bounded by 2ϵ . That is,

$$\left\| \mathcal{M}(\rho) - \sum_{j:|\omega_j| \leq 2} O_j \rho O_j^\dagger \right\|_1 \leq 2\epsilon. \quad (170)$$

Proof: [of Lemma 26] Recall that O_j is Hermitian. From Lemma 21 we have for any $w_j \in [-2, 2]$,

$$\|O_j - \sqrt{h}g_\gamma(w_j - O)\| \leq \delta(\gamma, h) := \delta. \quad (171)$$

Recall that in Algorithm 2, j takes values as $0, 1, \dots, N-1$, thus the size of the set $|\{j : |w_j| \leq 2\}| \leq N$. We have that we have that

$$\left\| \sum_{j:|w_j| \leq 2} O_j^2 - \sum_{j:|w_j| \leq 2} h g_\gamma^2(w_j - O) \right\| \quad (172)$$

$$\leq \left\| \sum_{j:|w_j| \leq 2} O_j (O_j - \sqrt{h}g_\gamma(w_j - O)) \right\| + \left\| \sum_{j:|w_j| \leq 2} (O_j - \sqrt{h}g_\gamma(w_j - O)) \sqrt{h}g_\gamma(w_j - O) \right\| \quad (173)$$

$$\leq N\delta + N\delta\sqrt{h} \frac{1}{\sqrt{\gamma\sqrt{2\pi}}} \quad (174)$$

$$\leq \epsilon. \quad (175)$$

Where in Eq. (173) we use $\|O_j\| \leq 1$ since O_j is a Kraus operator of a quantum channel. Recall that $\|O\| \leq 1$. Note that for any scalar $E \in [-1, 1]$, we have that

$$\sum_{j:|w_j| \leq 2} h g_\gamma^2(w_j - E) \geq \sum_{j:w_j \in [-1, 1]} h g_\gamma^2(w_j) = \sum_{k:k=-1/h}^{1/h} h g_\gamma^2(kh), \quad (176)$$

By the Fast convergent Riemann sum, i.e., Lemma 28 and Lemma 29, we have that

$$\left| \sum_{k:k=-1/h}^{1/h} h g_\gamma^2(kh) - 1 \right| \leq 4(2\sqrt{2\pi}\gamma)^{1/2} e^{-4\pi^2\gamma^2/h^2} + \frac{1}{\sqrt{\gamma\sqrt{2\pi}}}(h + \gamma^2)e^{-\frac{1}{2\gamma^2}} \leq \epsilon \quad (177)$$

Thus

$$\left\| \mathcal{M}(\rho) - \sum_{j:|\omega_j| \leq 2} O_j \rho O_j^\dagger \right\|_1 = \left\| \sum_{j:|w_j| > 2} O_j \rho O_j^\dagger \right\|_1 = \text{tr} \left(\sum_{j:|w_j| > 2} O_j \rho O_j^\dagger \right) \leq \left\| \sum_{j:|w_j| \leq 2} O_j^2 - I \right\| \leq 2\epsilon \quad (178)$$

■

Lemma 27 For any square matrix A, B we have that

$$\|[e^A, B]\|_1 \leq e^{\|A\|} \| [A, B] \|_1 \quad (179)$$

Proof: One can check that the following commutator identity holds.

$$[A^k, B] = \sum_{j=0}^{k-1} A^j [A, B] A^{k-1-j}, \quad (180)$$

Consider the Taylor expansion of e^A and apply inequality $\|MN\|_1 \leq \|M\|_1 \|N\|$, we have that

$$\|[e^A, B]\|_1 \leq \sum_{k=1}^{\infty} \frac{1}{k!} \sum_{j=0}^{k-1} \|A\|^j \|[A, B]\|_1 \|A\|^{k-1-j} = e^{\|A\|} \|[A, B]\|_1. \quad \blacksquare$$

Now, we are ready to prove Proposition 25.

Proof: [of the commutativity property] Recall that O_j is Hermitian. Recall that in Algorithm 2, j takes values as $0, 1, \dots, N-1$, thus the size of the set $|\{j : |w_j| \leq 2\}| \leq N$. By Lemma 26 we have that $\|\sum_{j:|w_j|\leq 2} O_j^2 - I\| \leq 2\epsilon$, thus

$$\|\mathcal{M}(\rho) - \rho\|_1 = \left\| \sum_{j:|w_j|\leq 2} [O_j, \rho] O_j \right\|_1 + 4\epsilon \quad (181)$$

$$\leq N \max_{j:|w_j|\leq 2} \|[O_j, \rho]\|_1 + 4\epsilon \quad (182)$$

where in the last inequality we use the fact that the number of j is bounded by N , and the norm $\|O_j\|$ is bounded by 1 since O_j is a Kraus operator of a quantum channel.

By Lemma 21, we have that for any j such that $w_j \in [-2, 2]$,

$$\|O_j - \sqrt{h}g_\gamma(\omega_j - O)\| \leq \delta, \quad (183)$$

For $|w_j| \leq 2$, we have that $\|w_j - O\| \leq 3$ since $\|O\| \leq 1$. Let $A_j := -\frac{(\omega_j - O)^2}{4\gamma^2}$. Then $\|A_j\| \leq \frac{9}{4\gamma^2}$. Moreover,

$$\|[A_j, \rho]\|_1 = \frac{1}{4\gamma^2} \|[(\omega_j - O)^2, \rho] \|_1 \quad (184)$$

$$= \frac{1}{4\gamma^2} \|- 2\omega_j [O, \rho] + [O^2, \rho]\|_1 \quad (185)$$

$$\leq \frac{1}{4\gamma^2} \left(2|\omega_j| \|[O, \rho]\|_1 + \|O[O, \rho] + [O, \rho]O\|_1 \right) \quad (186)$$

$$\leq \frac{1}{4\gamma^2} \left(2|\omega_j| \|[O, \rho]\|_1 + 2\|O\| \|[O, \rho]\|_1 \right) \leq \frac{3}{2\gamma^2} \|[O, \rho]\|_1. \quad (187)$$

Thus by Lemma 27 we have that

$$\|\mathcal{M}(\rho) - \rho\|_1 \leq 4\epsilon + N\sqrt{h} \frac{1}{\sqrt{\gamma\sqrt{2\pi}}} \max_{j:|w_j|\leq 2} \left\| \left[\exp\left(-\frac{(\omega_j - O)^2}{4\gamma^2}\right), \rho \right] \right\|_1 + N2\delta\|\rho\|_1 \quad (188)$$

$$\leq 4\epsilon + N\sqrt{h} \frac{1}{4\gamma^2\sqrt{\gamma\sqrt{2\pi}}} \exp\left(\frac{3}{4\gamma^2}\right) \|[O, \rho]\|_1 + N2\delta \quad (189)$$

$$\leq \epsilon^{-1} \text{poly log}(\epsilon^{-1}) \|[O, \rho]\|_1 + 5\epsilon. \quad (190)$$

where we use the fact that γ^{-1} is chosen to be $\mathcal{O}(\log^{1/2}(\epsilon^{-1}))$ thus $\exp(\frac{3}{4\gamma^2}) \leq \epsilon^{-1}$. \blacksquare

D.3.5 Technical lemmas for numerical analysis

Lemma 28 (Fast convergent Riemann sum) *Let $\varphi(x)$ be an integrable function (i.e., $\varphi \in L^1(\mathbb{R})$) with Fourier transform $\widehat{\varphi}(y) := \int_{-\infty}^{\infty} e^{-2\pi ixy} \varphi(x) dx$. Then, for $N \in \mathbb{Z}^+$ and $h > 0$, we have*

$$\left| h \sum_{k=-N/2}^{N/2-1} \varphi(kh) - \int_{-\infty}^{\infty} \varphi(x) dx \right| \leq \sum_{n=-\infty, n \neq 0}^{\infty} |\widehat{\varphi}(n/h)| + h \sum_{|k| \geq N/2} |\varphi(kh)|. \quad (191)$$

Proof: First, by the Poisson summation formula [41, Theorem 4.2.2], we have

$$h \sum_{k \in \mathbb{Z}} \varphi(kh) = \sum_{n \in \mathbb{Z}} \widehat{\varphi}(n/h). \quad (192)$$

Note that $\widehat{\varphi}(0) = \int_{-\infty}^{\infty} \varphi(x) dx$. Eq. (191) follows from the triangle inequality. \blacksquare

Lemma 29 (Gaussian sum) *Let $N \in \mathbb{Z}^+$ be an even integer and $A > 0$ be a positive scalar. Then, we have*

$$\sum_{k \geq N/2} e^{-Ak^2} \leq \left(1 + \frac{1}{AN}\right) e^{-AN^2/4}. \quad (193)$$

Proof: This summation can be upper-bounded by a Gaussian integral:

$$\begin{aligned} \sum_{k \geq N/2} e^{-Ak^2} &= e^{-AN^2/4} + \sum_{k=N/2+1}^{\infty} e^{-Ak^2} \leq e^{-AN^2/4} + \int_{N/2}^{\infty} e^{-Ax^2} dx \\ &\leq e^{-AN^2/4} + \frac{1}{N/2} \int_{N/2}^{\infty} x e^{-Ax^2} dx \leq \left(1 + \frac{1}{AN}\right) e^{-AN^2/4}. \end{aligned}$$

\blacksquare

References

- [1] M. H. Amin, E. Andriyash, J. Rolfe, B. Kulchytskyy, and R. Melko, “Quantum boltzmann machine,” *Physical Review X*, vol. 8, no. 2, p. 021050, 2018.
- [2] N. Wiebe and L. Wossnig, “Generative training of quantum boltzmann machines with hidden units,” *arXiv preprint arXiv:1905.09902*, 2019.
- [3] C.-F. Chen, M. Kastoryano, F. G. Brandão, and A. Gilyén, “Efficient quantum thermal simulation,” *Nature*, vol. 646, no. 8085, pp. 561–566, 2025.
- [4] Z. Ding, B. Li, and L. Lin, “Efficient quantum gibbs samplers with kubo–martin–schwinger detailed balance condition,” *Communications in Mathematical Physics*, vol. 406, no. 3, p. 67, 2025.
- [5] P. Rall, C. Wang, and P. Wocjan, “Thermal state preparation via rounding promises,” *Quantum*, vol. 7, p. 1132, 2023.
- [6] J. Jiang and S. Irani, “Quantum metropolis sampling via weak measurement,” *arXiv preprint arXiv:2406.16023*, 2024.
- [7] K. Temme, T. J. Osborne, K. G. Vollbrecht, D. Poulin, and F. Verstraete, “Quantum metropolis sampling,” *Nature*, vol. 471, no. 7336, pp. 87–90, 2011.
- [8] A. Gilyén, C.-F. Chen, J. F. Doriguello, and M. J. Kastoryano, “Quantum generalizations of glauber and metropolis dynamics,” *arXiv preprint arXiv:2405.20322*, 2024.
- [9] Z. Ding, Y. Zhan, J. Preskill, and L. Lin, “End-to-end efficient quantum thermal and ground state preparation made simple,” *arXiv preprint arXiv:2508.05703*, 2025.
- [10] M. Hagan and N. Wiebe, “The thermodynamic cost of ignorance: thermal state preparation with one ancilla qubit,” *arXiv preprint arXiv:2502.03410*, 2025.
- [11] D. Hahn, R. Sweke, A. Deshpande, and O. Shtanko, “Efficient quantum Gibbs sampling with local circuits.” 2025.
- [12] A. Sokal, “Monte carlo methods in statistical mechanics: foundations and new algorithms, chap 6,” in *Functional integration: Basics and applications*, pp. 131–192, Springer, 1997.
- [13] W. R. Gilks, S. Richardson, and D. Spiegelhalter, *Markov chain Monte Carlo in practice*. CRC press, 1995.

- [14] D. A. Levin and Y. Peres, *Markov chains and mixing times*, vol. 107. American Mathematical Soc., 2017.
- [15] F. Cesi, G. Guadagni, F. Martinelli, and R. Schonmann, “On the two-dimensional stochastic ising model in the phase coexistence region near the critical point,” *Journal of statistical physics*, vol. 85, no. 1, pp. 55–102, 1996.
- [16] F. Martinelli, “Lectures on glauber dynamics for discrete spin models, chap 6 phase coexistence,” in *Lectures on probability theory and statistics: Ecole d’été de probabilités de saint-flour xxvii-1997*, pp. 93–191, Springer, 2004.
- [17] R. Gheissari and A. Sinclair, “Low-temperature ising dynamics with random initializations,” in *Proceedings of the 54th Annual ACM SIGACT Symposium on Theory of Computing*, pp. 1445–1458, 2022.
- [18] A. Gelman and D. B. Rubin, “Inference from iterative simulation using multiple sequences,” *Statistical science*, vol. 7, no. 4, pp. 457–472, 1992.
- [19] D. Vats and C. Knudson, “Revisiting the gelman–rubin diagnostic,” *Statistical Science*, vol. 36, no. 4, pp. 518–529, 2021.
- [20] D. S. França, “Perfect sampling for quantum gibbs states,” *arXiv preprint arXiv:1703.05800*, 2017.
- [21] A. M. Dalzell, S. McArdle, M. Berta, P. Bienias, C.-F. Chen, A. Gilyén, C. T. Hann, M. J. Kastoryano, E. T. Khabiboulline, A. Kubica, et al., “Quantum algorithms: A survey of applications and end-to-end complexities (2023),” *arXiv preprint arXiv:2310.03011*.
- [22] L. Lin and Y. Tong, “Heisenberg-limited ground-state energy estimation for early fault-tolerant quantum computers,” *PRX quantum*, vol. 3, no. 1, p. 010318, 2022.
- [23] M. A. Nielsen and I. L. Chuang, *Quantum computation and quantum information*. Cambridge university press, 2010.
- [24] J. E. Moussa, “Low-depth quantum metropolis algorithm,” *arXiv preprint arXiv:1903.01451*, 2019.
- [25] C.-F. Chen, M. J. Kastoryano, and A. Gilyén, “An efficient and exact noncommutative quantum gibbs sampler,” *arXiv preprint arXiv:2311.09207*, 2023.
- [26] J. Goodman and J. Weare, “Ensemble samplers with affine invariance,” *Communications in applied mathematics and computational science*, vol. 5, no. 1, pp. 65–80, 2010.
- [27] M. B. Thompson, “A comparison of methods for computing autocorrelation time,” *arXiv preprint arXiv:1011.0175*, 2010.
- [28] S. Bravyi, A. Chowdhury, D. Gosset, and P. Wocjan, “On the complexity of quantum partition functions,” *arXiv preprint arXiv:2110.15466*, 2021.
- [29] A. Gilyén, Y. Su, G. H. Low, and N. Wiebe, “Quantum singular value transformation and beyond: exponential improvements for quantum matrix arithmetics,” in *Proceedings of the 51st annual ACM SIGACT symposium on theory of computing*, pp. 193–204, 2019.
- [30] A. M. Childs and N. Wiebe, “Hamiltonian simulation using linear combinations of unitary operations,” *arXiv preprint arXiv:1202.5822*, 2012.
- [31] G. H. Low and I. L. Chuang, “Hamiltonian simulation by qubitization,” *Quantum*, vol. 3, p. 163, 2019.
- [32] J. Haah, M. B. Hastings, R. Kothari, and G. H. Low, “Quantum algorithm for simulating real time evolution of lattice hamiltonians,” *SIAM Journal on Computing*, vol. 52, no. 6, pp. FOCS18–250, 2021.
- [33] C.-F. Chen and C. Rouzé, “Quantum gibbs states are locally markovian,” *arXiv preprint arXiv:2504.02208*, 2025.

- [34] A. M. Childs, R. Kothari, and R. D. Somma, “Quantum algorithm for systems of linear equations with exponentially improved dependence on precision,” *SIAM Journal on Computing*, vol. 46, no. 6, pp. 1920–1950, 2017.
- [35] J. Jiang, X. Sun, S.-H. Teng, B. Wu, K. Wu, and J. Zhang, “Optimal space-depth trade-off of cnot circuits in quantum logic synthesis,” in *Proceedings of the Fourteenth Annual ACM-SIAM Symposium on Discrete Algorithms*, pp. 213–229, SIAM, 2020.
- [36] A. M. Childs, “Lecture notes on quantum algorithms,” *Lecture notes at University of Maryland*, vol. 5, 2017.
- [37] A. Kitaev and W. A. Webb, “Wavefunction preparation and resampling using a quantum computer,” *arXiv preprint arXiv:0801.0342*, 2008.
- [38] M. M. Wolf, “Quantum channels and operations-guided tour,” 2012.
- [39] K. Temme, M. J. Kastoryano, M. B. Ruskai, M. M. Wolf, and F. Verstraete, “The χ^2 -divergence and mixing times of quantum markov processes,” *Journal of Mathematical Physics*, vol. 51, no. 12, 2010.
- [40] L. Grover and T. Rudolph, “Creating superpositions that correspond to efficiently integrable probability distributions,” *arXiv preprint quant-ph/0208112*, 2002.
- [41] M. A. Pinsky, *Introduction to Fourier analysis and wavelets*, vol. 102. American Mathematical Society, 2023.